JAERI-M
8503

ENGINEERING ASPECTS OF THE JAERI PROPOSAL FOR INTOR (I)

October 1979

Kiyoshi SAKO, Tatsuzo TONE, Yasushi SEKI, Hiromasa IIDA
Harumi YAMATO[*1], Koichi MAKI[*2], Kimihiro IOKI[*3],
Takashi YAMAMOTO[*4], Akio MINATO[*5], Hiromi SAKAMOTO[*6],
Kichiro SHINYA[*1]

日本原子力研究所
Japan Atomic Energy Research Institute

この報告書は，日本原子力研究所が JAERI-M レポートとして，不定期に刊行している研究報告書です．入手，複製などのお問合わせは，日本原子力研究所技術情報部（茨城県那珂郡東海村）あて，お申しこしください．

JAERI-M reports, issued irregularly, describe the results of research works carried out in JAERI. Inquiries about the availability of reports and their reproduction should be addressed to Division of Technical Information, Japan Atomic Energy Research Institute, Tokai-mura, Naka-gun, Ibaraki-ken, Japan.

JAERI- M 8503

Engineering Aspects of the JAERI Proposal for INTOR (I)

K. SAKO, T. TONE, Y. SEKI, H. IIDA,
H. YAMATO*1, K. MAKI*2, K. IOKI*3, T. YAMAMOTO*4,
A. MINATO*5, H. SAKAMOTO*6, K. SHINYA*1

Division of Thermonuclear Fusion Research
Tokai Research Establishment, JAERI

(Received June , 1979)

A design study of INTOR has been carried out in order to evaluate the validity of the guiding design parameters and also to demonstrate the feasibility of installing the tritium breeding blanket.

The engineering issues were evaluated of the two concepts proposed for impurity control and ash exhaust, namely, a concept with poloidal divertors and a non-divertor concept. As a result of a preliminary study, the following findings have been obtained.

1) Some of the guiding parameters of INTOR are severe to the engineering and leave only small margin, but a concept satisfying the parameters is feasible. In that sense, the guiding parameters may be considered appropriate.
2) Tritium breeding blanket (Helium cooled Li_2O blanket) with the breeding ratio greater than 0.5 is shown to be feasible in the case without divertor. The ratio of 0.4 is possible for the case with divertors.

Keywords: INTOR Tokamak Reactor, Guiding Parameters, Divertor, Non-divertor, Design Study, Tritium Breeding, Helium Cooling, Lithium Oxide Blanket

---

*1 On leave from Tokyo Shibaura Electric Co. Ltd., Kasawaki, Japan
*2 On leave from Hitachi, Ltd., Tokyo, Japan
*3 On leave from Mitsubishi Atomic Power Industries Inc., Omiya, Japan
*4 On leave from Fuji Electric Co. Ltd., Kawasaki, Japan
*5 On leave from Kawasaki Heavy Industries, Ltd., Tokyo, Japan
*6 On leave from Mitsubishi Heavy Industries, Ltd., Kobe, Japan

This report was presented at the Session 2 of IAEA INTOR Workshop held in Vienna, June, 11 - July 6, 1979.

トカマク型核融合炉INTORの工学的諸問題の検討（I）

日本原子力研究所東海研究所核融合研究部

迫　　淳・東稔　達三・関　　泰・飯田　浩正

大和　春海[*1]・真木　紘一[*2]・伊尾木公裕[*3]・山本　　孝[*4]

湊　　章男[*5]・坂本　寛己[*6]・新谷　吉郎[*1]

（1979年6月受理）

現在，IAEA主催による次期トカマク型核融合炉（INTOR）の国際共同設計・建設を目ざしたワークショップにおいて，炉概念及び設計の指針の作成作業が進められている。このレポートでは，INTORの設計条件に基づいて設計を行い，その指針パラメータの妥当性とトリチウムブランケットの設置の可能性について検討した結果を報告する。

日本が不純物制御と灰の排気の観点から提案した2つの炉概念，即ちポロイダル・ダイバータ付の場合とダイバータなしの場合について予備設計を行い，その結果次のことが明らかになった。

1) INTORの設計条件の中には工学上かなり厳しく余裕のないものもあるが，設計条件を満す炉概念は不可能でない。

2) トリチウム増殖比に関しては，He冷却によるLi_2Oブランケットの採用によって，ダイバータなしの場合で0.5以上，ダイバータ付の場合で0.4を得ることが可能である。

*1 外来研究員：東京芝浦電気K.K.

*2 〃　：日立製作所

*3 〃　：三菱原子力工業K.K.

*4 〃　：富士電機製造K.K.

*5 〃　：川崎重工業K.K.

*6 〃　：三菱重工業K.K.

CONTENTS

目　　次

1. General

A design study has being conducted in order to evaluate the validity of the guiding parameters of INTOR and also to verify the feasibility to load the tritium breeding blankets. The engineering study about the tokamak machine are enumerated in the following and some descriptive figures are shown in Figs. 1.1∿1.4. Major parameters related to this design are summarized in Table 1.1.

1. Overall design study
2. Nuclear heating rate distribution
3. Neutron and gamma ray flux distribution
4. Tritium production rate distribution
5. Shielding capability
6. Location of vacuum boundary
7. First wall (cooling panel with protection wall) thermal and structural analysis
8. Thermal and structural analysis of inner blanket
9. Tritium breeding blanket thermal and structural analysis
10. Shielding structure analysis
11. Concept study of toroidal field magnet
12. Concept study of poloidal field magnet
13. Concept study of neutral beam injector
14. Cooling system and power generating system for blanket and cooling panel
15. Thermal analysis of divertor plate
16. Repair and maintenance

As a result of the above study, the following conclusions have been obtained.

1) Some of the guiding parameters of INTOR are severe to the engineering and leave only small margin in some cases, but a concept satisfying the parameters is feasible. In that sense, they may be considered appropriate.

2) Tritium breeding blanket (He cooled Li_2O blanket) with the breeding ratio greater than 0.5 is shown to be feasible in the case without divertor. It can reach about 0.4 in the case with divertors.

The complexity induced by the introduction of the breeding blanket seems tolerable. The required blower power for the blanket system can fully be supplied by the electricity generated by INTOR itself.

3) The choice of repair and maintenance scheme greatly influences the concept of the reactor itself and the reactor building. Therefore, fairly detailed design study must be conducted at the early stage in order to determine the repair and maintenance scheme. (The bore of the toroidal field magnets must be enlarged if a certain repair and maintenance scheme is to be adopted.) Module extraction scheme has been studied in detail for JAERI Experimental Fusion Reactor (JXFR)[1]

Reference

1) K. Sako, T. Tone, Y. Seki, H. Iida, H. Yamato et al.; Second Preliminary Design of JAERI Experimental Fusion Reactor (JXFR) [Interim Report], JAERI-M 8286 (1979).

Table 1.1 DESIGN PARAMETERS

basic parameters	
average neutron wall loading	1 MW/m^2
fusion power	395 MW
total-thermal power	436 MW
burn time	200 s
dwell time	100 s
availability	25 %
number of pulses during lifetime	3×10^5
major radius (R)	5.0 m
aspect ratio (A)	4.2
plasma radius (r_{plasma})(z=0)	1.2 m
wall radius (r_{wall}) (z=0)	1.3 m
elongation	1.5
toroidal magnetic field at axis (B_{TO})	5 T
plasma current	4.7 MA
field ripple	$\pm$ 0.75 %
heating	
power	$\sim$ 50 ($\sim$ 70) MW
duration	$\sim$ 5 s
mode	NBI
neutral beam energy	200 keV
toroidal field coils	
number	12
conductor	Nb_3Sn
bore, height/width	9 m/ 6 m
pulsed field	0.1 $\sim$0.2 T/s
radiation	$\sim 8 \times 10^8$ rad (epoxy)
poloidal field coils* (hybrid coil system)	
OH current ramp time	$\sim$ 5 s
OHC conductor	SC
OHC location	outside B_t coil
OHC max. field	$\pm$ 6 T
OHC max. field rise	$\sim$ 4 T/s ($t \leq 0.1$ s)
	$\sim$ 1 T/s ($0.1 \leq t \leq 5$ s)
EFC conductor	SC/Cu
EFC location	outside B_t coil

(continued)

DFC conductor	SC
DFC location	outside B_t coil
divertor field	spatially depending
BDC conductor	
BDC location	
max. one-turn voltage	∿100 V

vacuum vessel

location-primary vessel	inner surface of bulk shield
material	stainless steel
max. temperature	∿150°C
coolant	H_2O
toroidal loop resistance	0.2 mΩ

first wall

type	cooling panel with protection wall protection wall	cooling panel
thickness/outer dia.	∿5 mm	2 mm/20 mm
material	low Z mat. or low Z covered refractory metal	316 SS
coolant	none (by radiation)	He pressure: 70 ata temperature {inlet : 200°C {outlet : 300°C
max. temp.-structure	∿1500°C	∿400°C

av. neutron wall load (during burn)	1 MW/m^2
av. surface heat load (" ")	0.25 MW/m^2 ∿ 0.3 MW/m^2

number of disruptions/life time	to be determined
toroidal loop resistance	see vacuum vessel
electric power	17 MW(gross)
	11 MW(net)

blanket (non-breeding)

number of modules	6
location	inboard only
material	316 SS
coolant	H_2O

(continued)

max. temp. (structure)	∿ 200°C
thickness	0.3 m
poloidal field response time	to be determined
blanket (T-breeding)	
breeding ratio	∿ 0.5 (non-divertor)
number of modules	6
type	cellular type
location	outboard only
material, structural	316 SS
material, breeding	Li_2O
coolant	He pressure : 30 ata temperature inlet : 250°C outlet: 550°C
max. temperature (structure)	∿ 400°C
electric power	36 MW (gross) 32 MW (net)
bulk shield	
inboard material	SS and W-alloy
inboard thickness	0.4 m(0.7 m, including inner blanket)
outboard material	SS
outboard thickness	1 m
coolant	H_2O/borated H_2O
max. temperature (structure)	∿ 150°C

*OHC: ohmic heating coils, EFC: equil. field coils, DFC: divertor field coils, BDC: breakdown field coils.

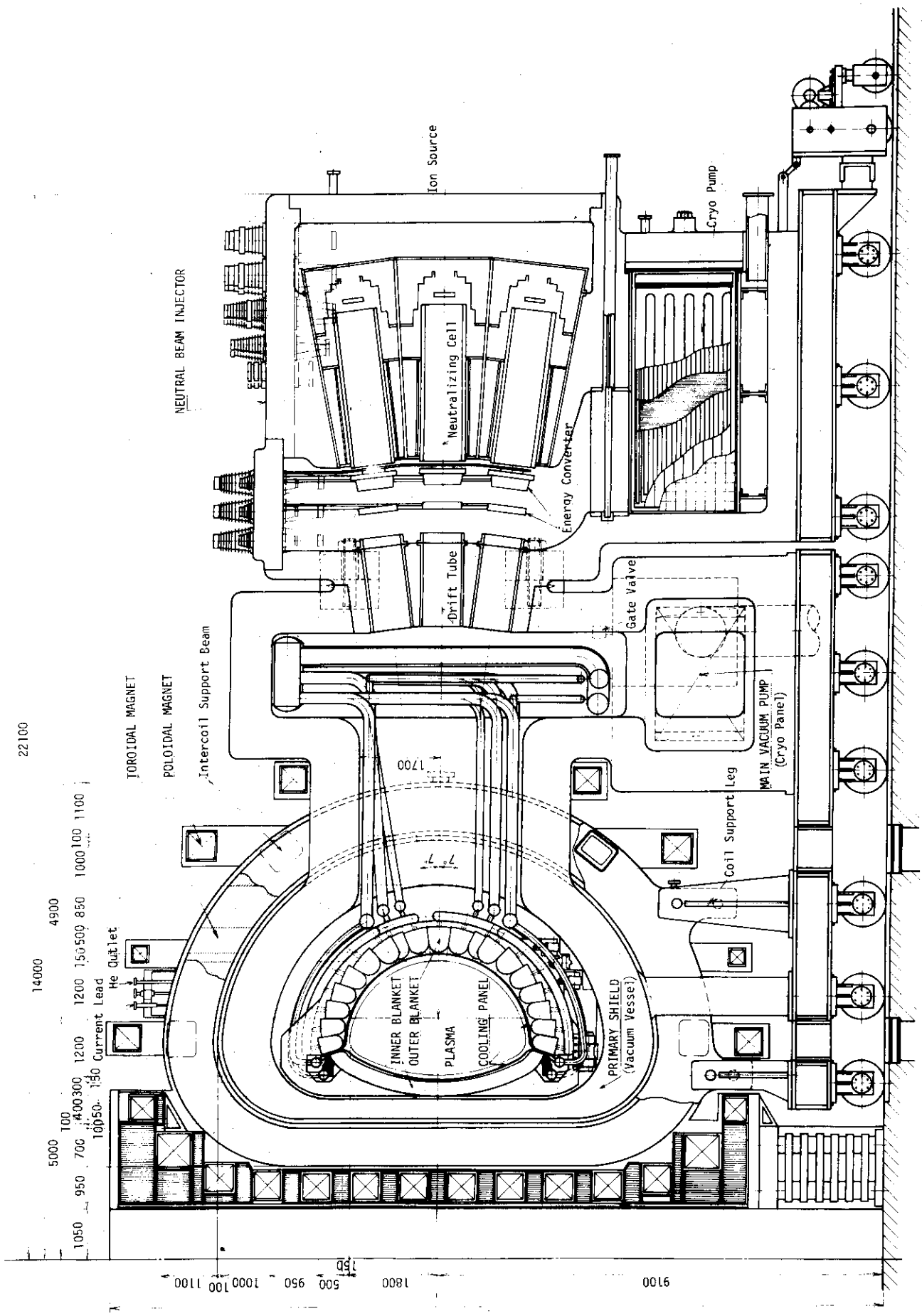

Fig.1.1 Vertical View of INTOR-J (Non Divertor)

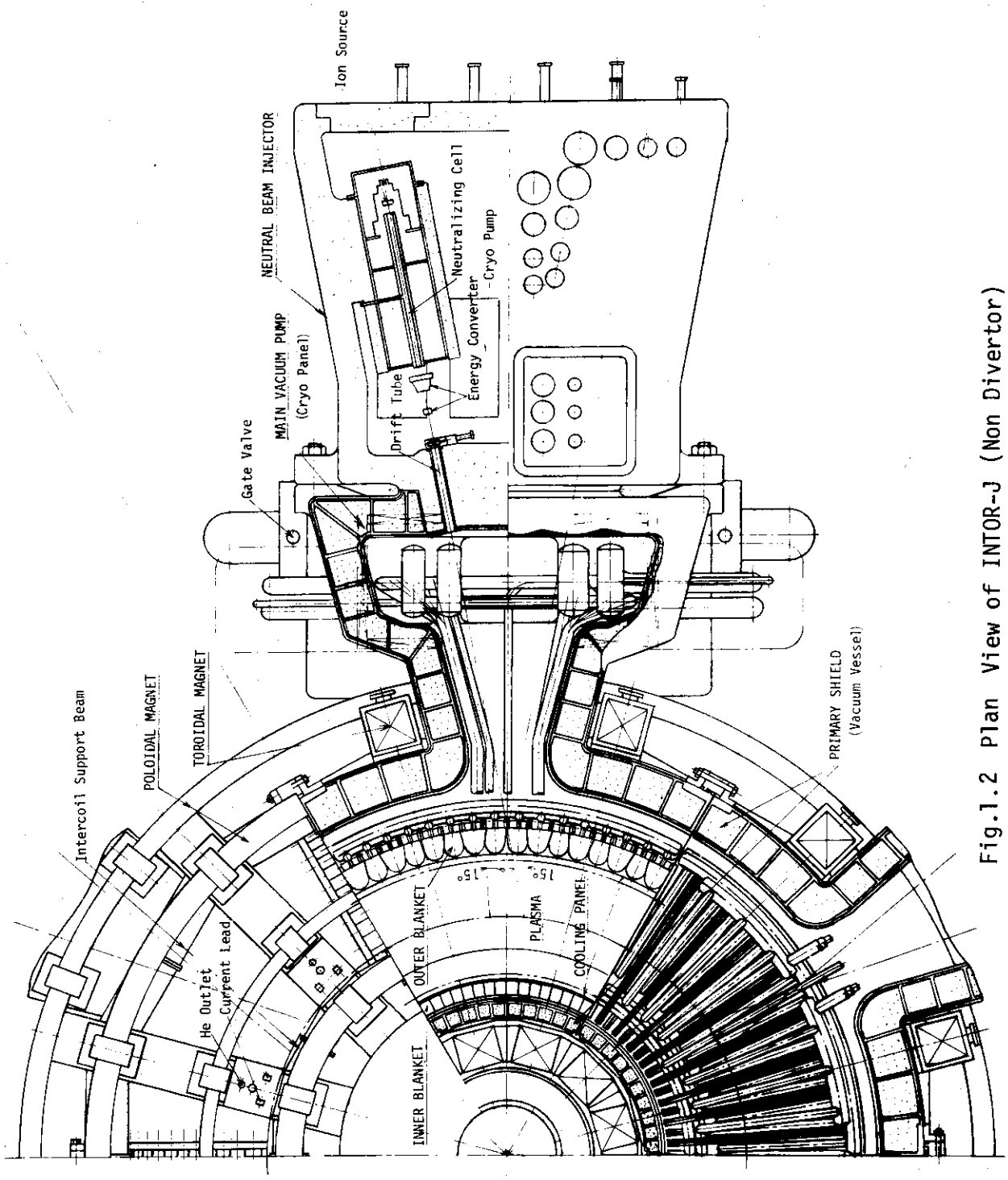

Fig.1.2 Plan View of INTOR-J (Non Divertor)

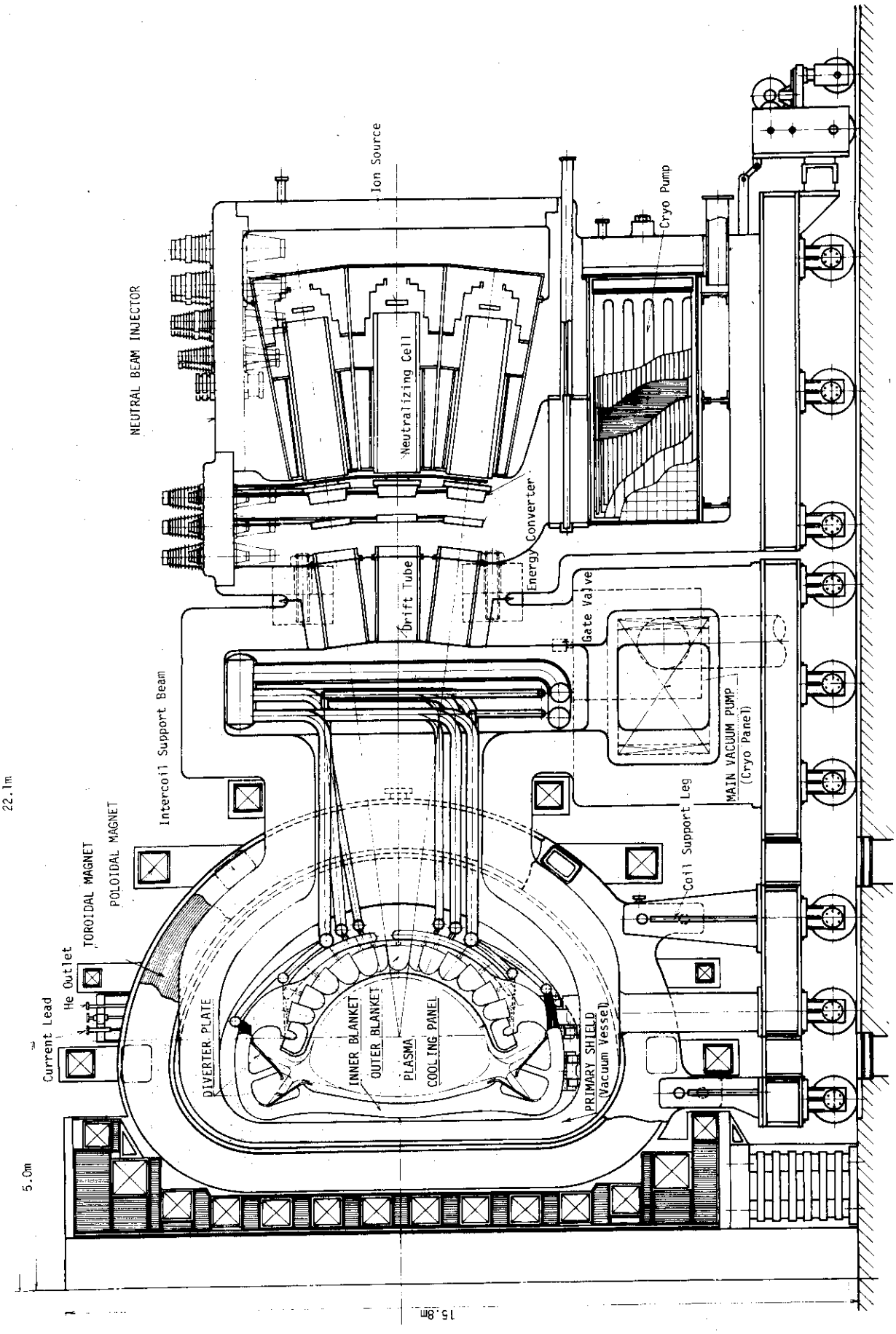

Fig.1.3 Vertical View of INTOR-J (With Divertor)

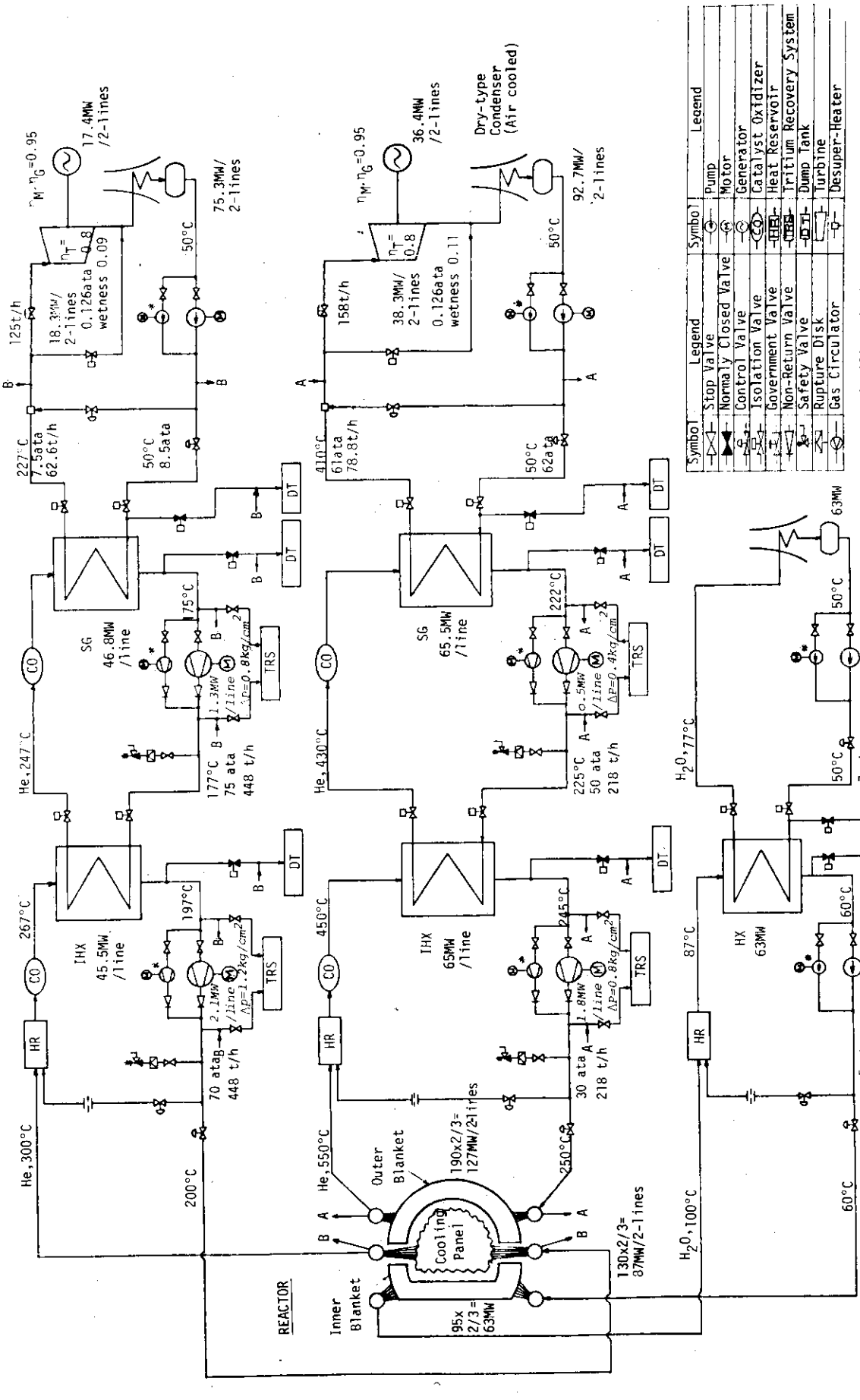

Fig.1.4 Flow Diagram of Cooling System of INTOR-J (Non Divertor)

2. Reactor Structure

Arrangement of the reactor components is shown in Figs. 1.1 and 1.2. The reactor consists of six reactor modules which may be withdrawn in the radial direction for repair. Each reactor module consists of two toroidal field magnets, one primary shield and one blanket module. Each blanket module consists of outer blanket (tritium breeding), inner blanket (non-breeding) and cooling panel and has a 1.6 x 1.0 m hole for the neutral beam injection and evacuation. Four injectors are alternately installed. Two vacuum pumps (cryo-pumps) are installed to every reactor module.

2.1 Blanket structure

A blanket structure shown in Fig.2.1.1 consists of 6 blanket modules and is placed in a vacuum vessel. Each module is divided into 16 blanket rings and is assembled with inner blanket (non tritium breeding), outer blanket (tritium breeding), cooling panel including a protection wall, piping system and support structure.

A cooling panel is provided at the plasma side in front of the inner and outer blanket. It is sustained with supporting bar which is attached to the blanket ring flanges.

The blanket cells are taken in a triangular arrangement in this design and are fixed with two ring flanges welded to the outside of the cover plate.

There are two kinds of the blanket rings for the sake of the triangular arrangement and they are assembled alternately. However, the two blanket rings which have a neutral beam injection hole is not taken in the triangular arrangement. Moreover, as the both end rings of the blanket module separate from the adjacent blanket modules, the triangular arrangement is not taken in these end rings.

The inner and outer blanket module is formed with ring units. The inner and outer blanket ring is connected with each ring flange to increase the strength of the blanket structure due to the unification of two ring flanges.

A piping system for the outer blanket is formed with a lot of blanket pipes, some collection manifolds, some inlet and outlet headers and main coolant pipes. The former two components are made of coaxial pipes with the hot outlet pipe inside the inlet pipe so that the piping arrangement becomes simple and the temperature of the blanket structure becomes low.

The thermal insulator is attached to the inside surface of the outlet pipe in order to avoid the thermal expansion of the outlet pipe and the heat exchange between inlet and outlet pipe.

In case of repair and maintenance, the blanket module will be withdrawn in the toroidal direction by using a wheel which is set on the lower part of the blanket module. In this case, the main pipe will be disconnected by automatic cutting machine. During operation, however, the blanket module will be supported with the support block which is set under the blanket module support.

The weights of the each component are as follows.

a.	blanket cells	55 ton/module
b.	inner blanket	32 ton/module
c.	cooling panel	5 ton/module
d.	piping header	34 ton/module
e.	ring flange	47 ton/module
f.	support structure	10 ton/module
	total	183 ton/module

2.1.1 Outer Blanket(Blanket Cell)

Fig.2.1.2 shows a typical blanket cell. The blanket vessel is a double-walled and truncated conical thin shell made of Type 316 stainless steel with a spherical domed surface at the plasma side. A thick cover plate to which inlet and outlet coaxial duct attached is placed at the opposite side of the plasma. Ribs (5 x 5 mm) for the coolant channel are provided between inner and outer wall. For tritium breeding, the blanket cell contains pebbles and blocks of lithium oxide (Li_2O) which are packed in the stainless steel canning to prevent their deformations.

The blanket cell is cooled by a helium gas at 30 kgf/cm^2 during operation. The coolant flows helically between inner and outer wall and arrives at the plasma side. The coolant enters from the inlet duct at 250°C becomes about 340°C at the top of the dome and exits from outlet duct at 550°C being heated in the inner part (Li_2O) of the blanket cell. The temperature on the top of the dome is about 370°C (See Fig. 2.1.5).

The blanket cell are fixed with two pieces of ring flanges welded to the outside of the cover plate as shown in Fig.2.1.2.

2.1.2 Inner Blanket (Non Tritium Breeding)

An inner blanket shown in Fig.2.1.3 is made of 30 cm thick stainless steel which is curved along a plasma face. The inner blanket is formed with 6 inner blanket modules and each module consists of 16 inner blanket blocks and they are fixed with two pieces of flanges welded to each block. The block is divided into 20 plates in the radial direction and some cooling tubes are put between two plates as shown in Fig.2.1.3 In order to enhance the thermal conductivity of the gap between the cooling tube and the hole of the block, the cooling tube will be brazed to the inside of the hole.

A thermal energy generated in the block is removed with pressurized water which flows in the cooling tube. The coolant enters from the inlet header which is provided at the lower part of the blanket structure and exits from the outlet header (collecting the coolant) which is provided at the upper part of the blanket structure.

The temperature of the inlet and outlet coolant are 60°C and 100°C, respectively. The maximum temperature of the inner blanket structure is about 185°C. The velocity and pressure of the coolant are 1.22m/sec and 5 ata, respectively.

The thermal energy generated in the inner blanket is about 95 MW and is not used for the generation of the electric power.

The thermal energy generated in the inner blanket is about 95 MW and is not used for the generation of the electric power. Helium cooling of the inner blanket was precluded from the lack of space in the vacuum chamber for the complex helium cooling piping structure. Therefore water cooling was selected. This selection was not made from the viewpoint of improving the neutron shielding capability.

2.1.3 Stress Analysis of Blanket Vessel

The stress analysis of the blanket vessel which forms the outer blanket module for tritium breeding is carried out.

The blanket vessel is a double-walled and truncated conical thin shell with the spherical dome at the plasma side made by Type 316 stainless steel. The blanket vessel is cooled by a helium gas at 30 kgf/cm^2 during operation. The inlet and outlet temperature of the coolant are 250°C and 550°C, respectively. The maximum nuclear heating ratio is 11 W/cc at the top of the dome.

Fig.2.1.4 shows the calculational model for the outer wall of the blanket vessel. Two-dimensinal axisymmetric finite element was employed for the elastic and thermal stress analysis. The thickness of the body is 12 mm and the thickness of the dome is 6 mm at the top. The height for the coolant channel (5 mm) and the thickness of the inner wall (5 mm) were excluded from the those thickness and the thick cover plate was not considered in this analysis.

We carried out the stress analysis under internal pressure 30 kgf/cm^2 taking account of temperature distribution of the blanket vessel during burn time. The temperature distribution employed in this analysis was obtained from a steady state heat transfer analysis with two-dimensional model using above conditions, assuming that the temperature was constant in the circumferential direction of the outer wall as shown in Fig. 2.1.5. The material properties of Type 316 stainless steel at 400°C were used in this analysis. The Young's modulus E, Poisson's ratio ν and mean coefficient of thermal expansion α are 17200 kgf/mm^2, 0.3 and 1.8×10^{-5}/°C, respectively.

The pre and post deformations of the blanket vessel is shown in Fig.2.1.6. The distributions of the stress intensities at the inside and outside surface are shown in Fig.2.1.7. The maxima of the stress intensities at the inside and outside surface were 11.7 kgf/mm^2 and 6.5 kgf/mm^2, respectively.

Assuming that those stress intensities are taken for P_L+P_b+Q in ASME. Boiler and Pressure Vessel Code Sec.III, they are smaller than 3Sm (Sm is an allowable stress and is 11.3 kgf/mm^2 of Type 316 stainless steel at 400°C). Therefore,the blanket vessel has an enough margin against failure.

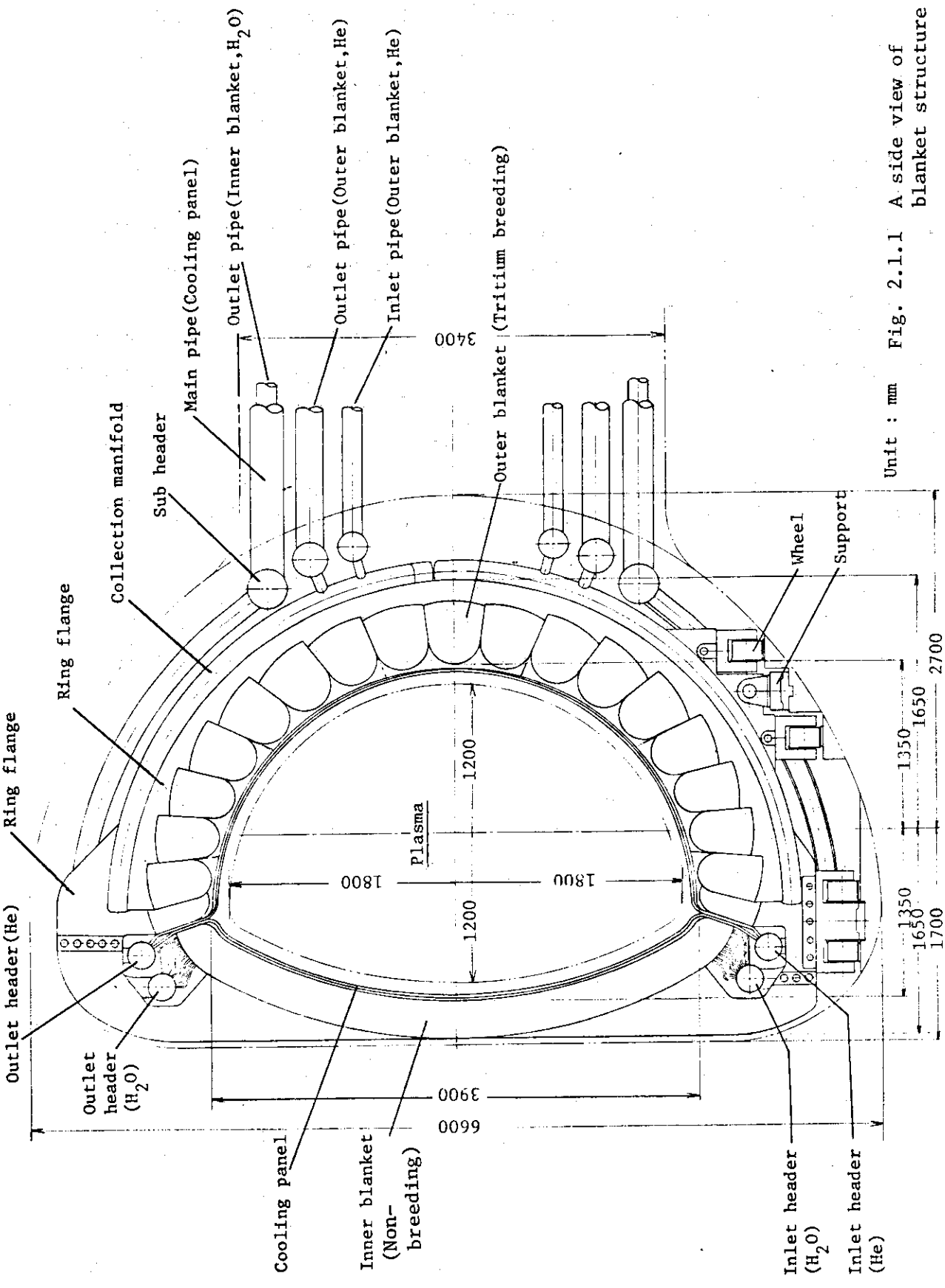

Unit : mm

Fig. 2.1.1 A side view of blanket structure

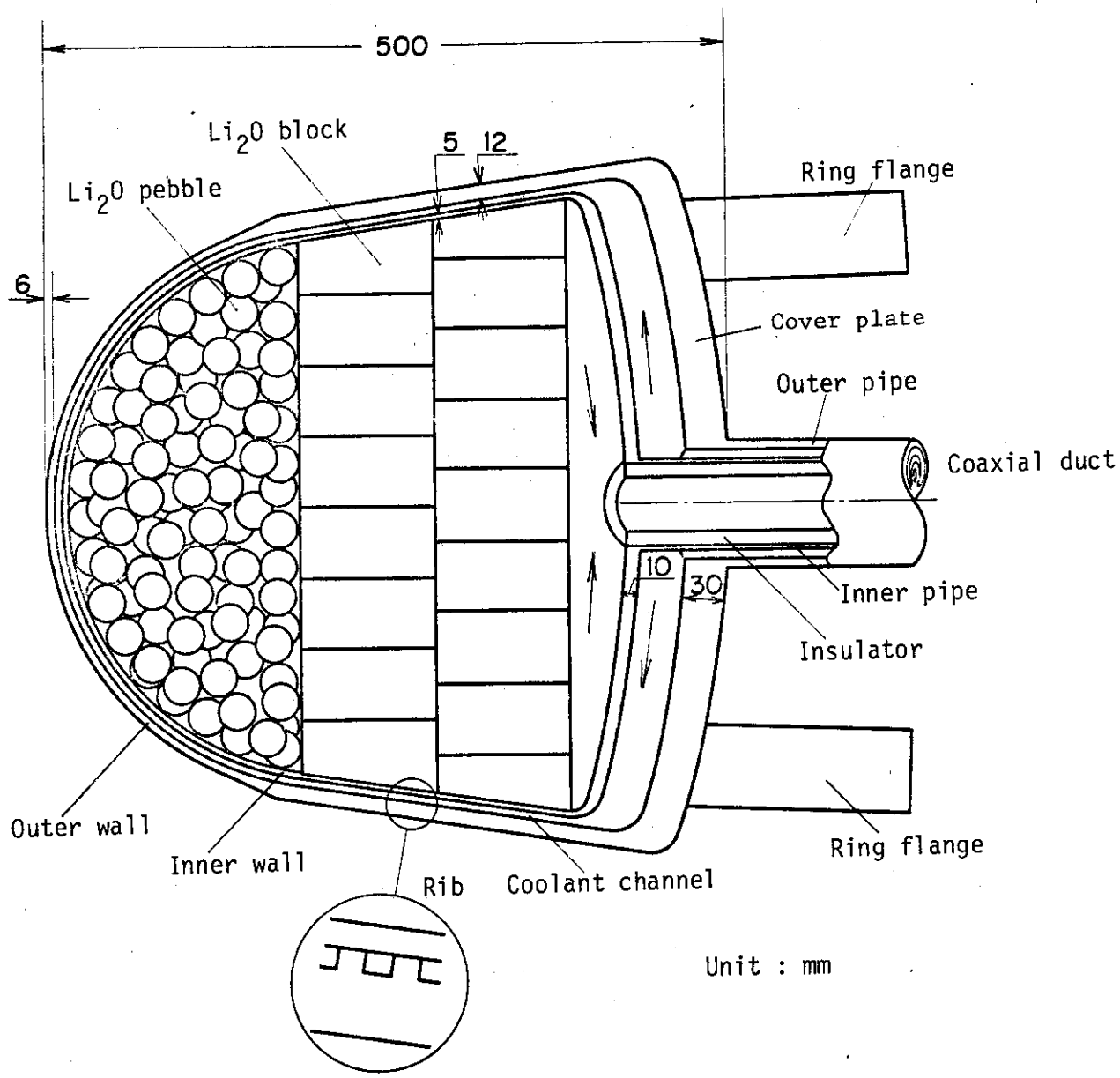

Fig.2.1.2 A typical blanket cell

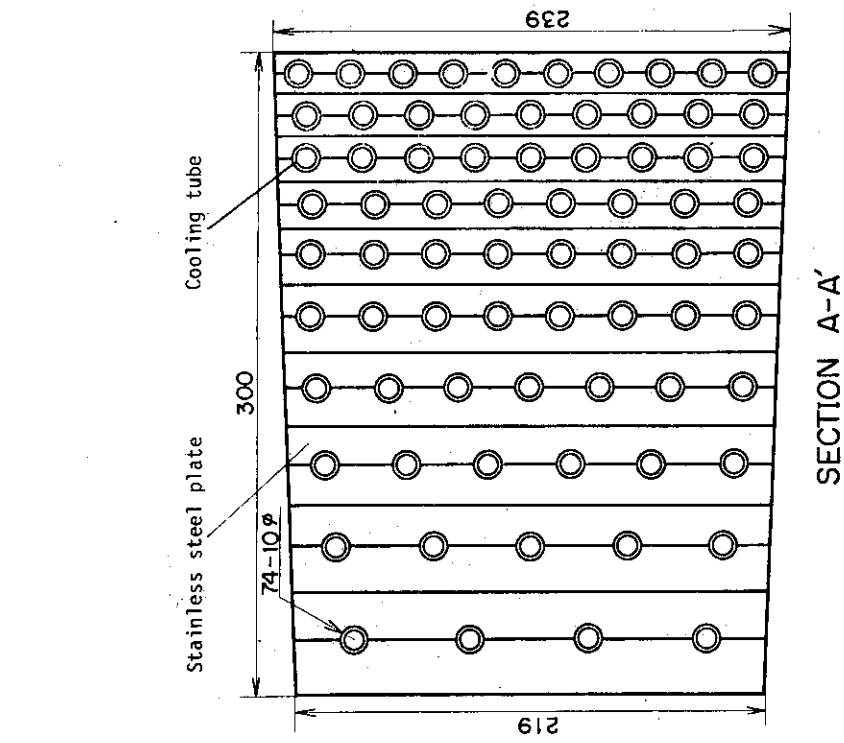

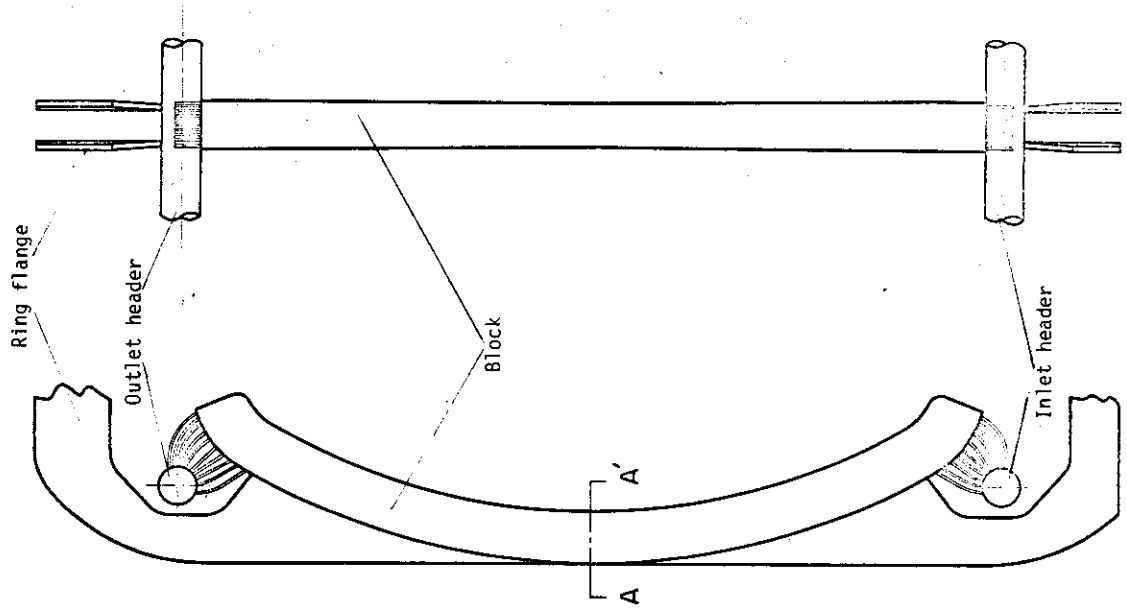

Fig.2.1.3 Inner blanket ring

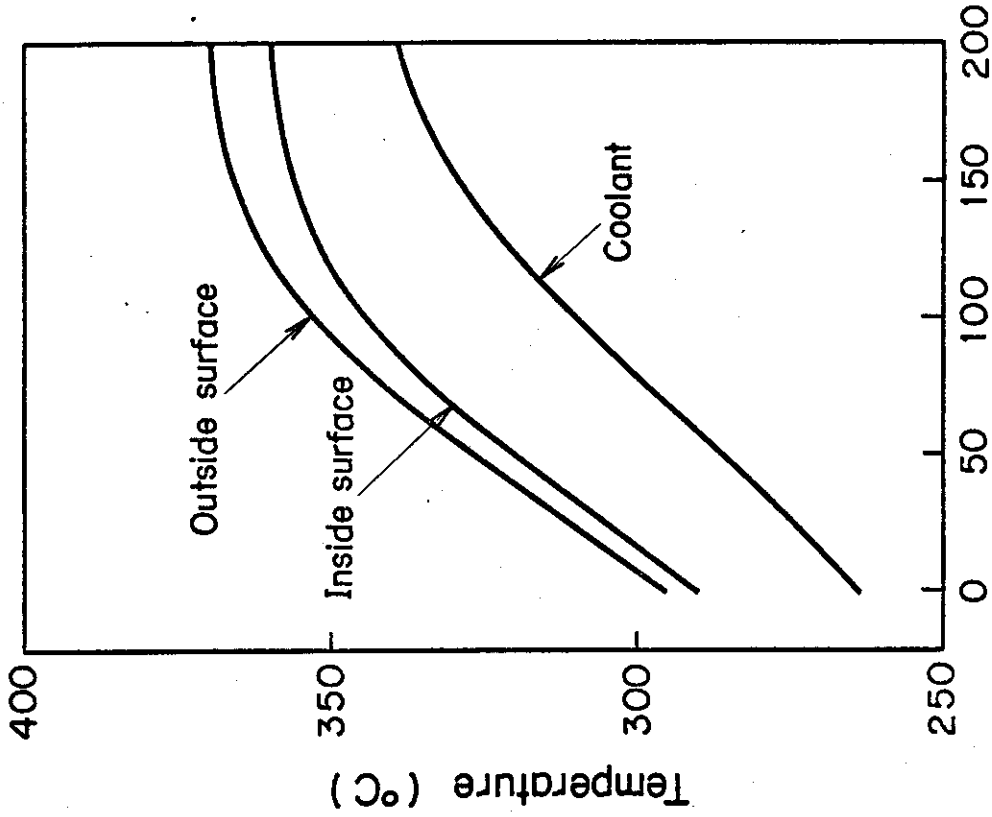

Fig.2.1.5 Temperature distribution at the dome of the blanket vessel

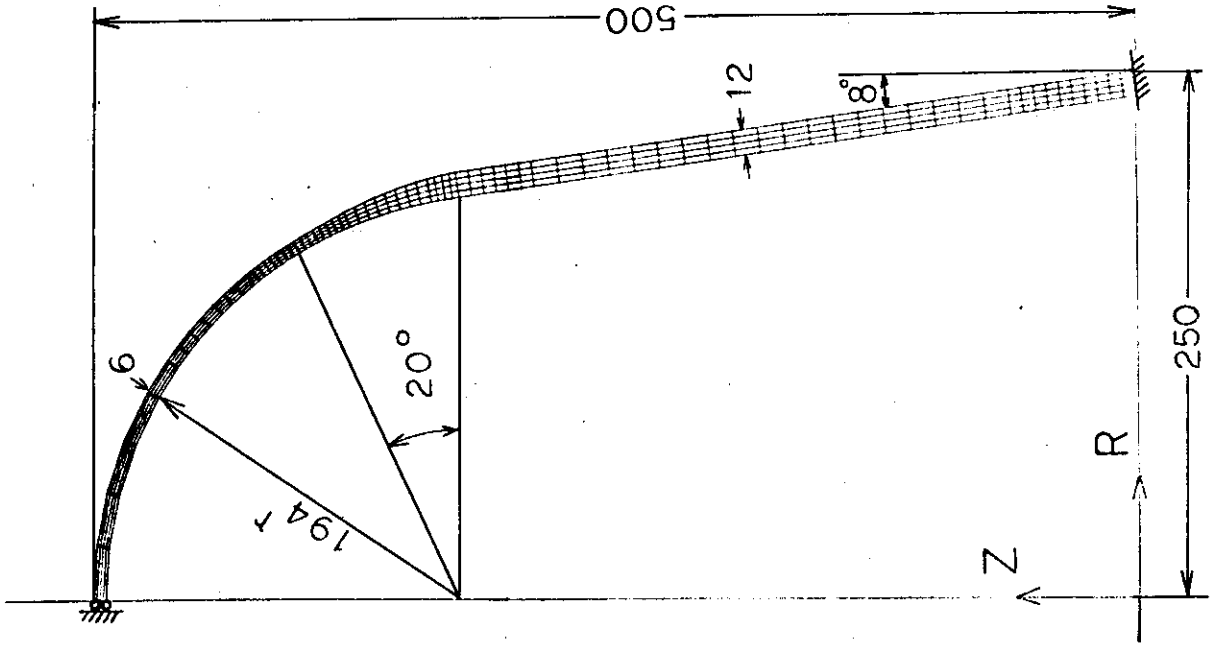

Fig.2.1.4 Calculational model and finite element mesh of the blanket vessel

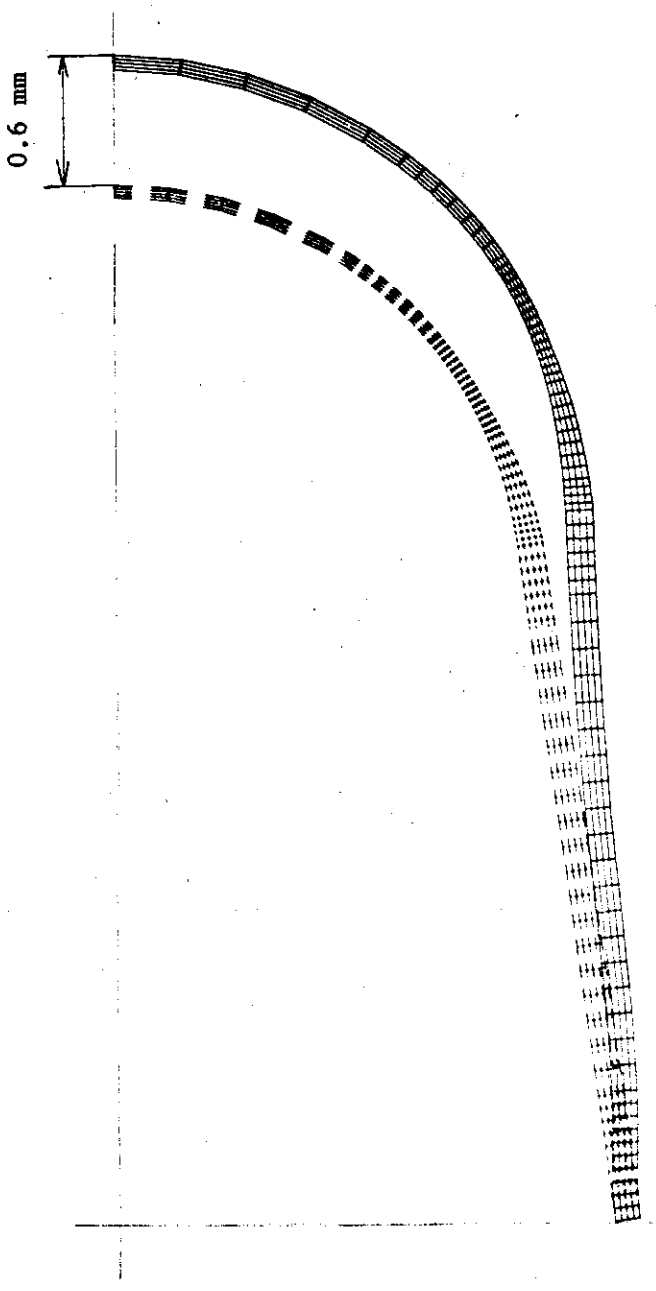

Fig.2.1.6 Exaggerated deformation shape of the blanket vessel

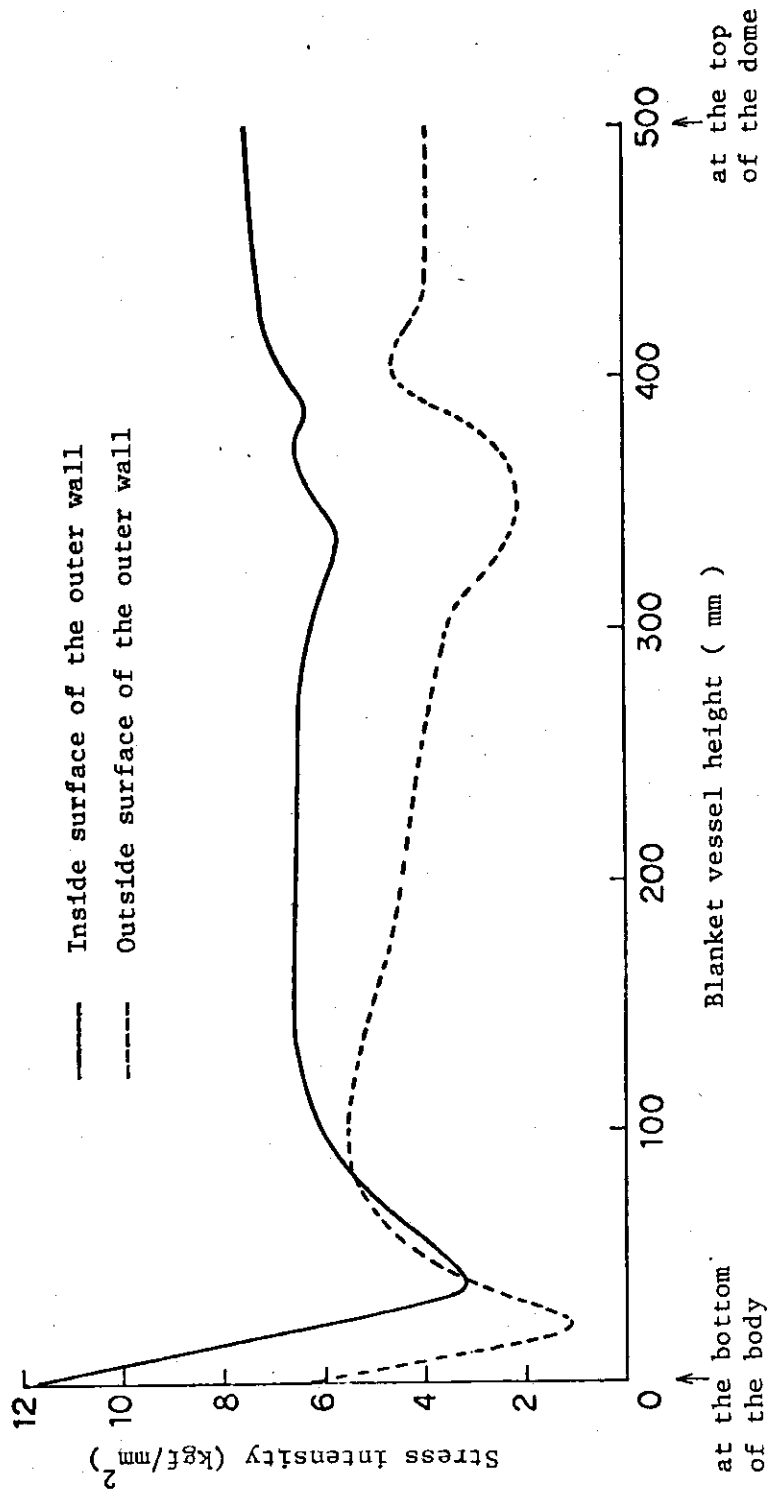

Fig.2.1.7 Distributions of the stress intensities of the blanket vessel under internal pressure and temperature distribution

2.2 Cooling panel

Fig.2.2.1 shows a cooling panel. The cooling panel is provided in front of the inner and outer blanket surrounding a plasma in order to remove all thermal radiation which comes from the plasma and nuclear heating. The cooling panel consists of 6 cooling panel modules and each module is formed with 16 cooling panel rings.

The cooling panel is a membrane wall structure which is assembled with a lot of fin-tubes having a small diameter made of Type 316 stainless steel.

A protection wall which is made of TZM is attached to the plasma side of the cooling fin-tube so that the plasma does not directly contacts with the surface of the cooling fin-tube. The shape of the protection wall is a semi-cylindrical shell which is determined from the following requirements, (1) to moderate the thermal radiation to the cooling panel and (2) to transfer the thermal radiation to the backside of the cooling panel.

The cooling panel is cooled by a helium gas at 70 ata. The coolant enters from the inlet header which is provided at the lower part of the torus, flows through the inside and outside surface of the torus and is collected with the outlet header at the upper part. The inlet and outlet temperature of the coolant are 200°C and 300°C,respectively and the maximum temperature of the structural material (pressure boundary) is about 400°C.

2.2.1 Thermal analysis

The heat flux to the first wall from plasma is 25 W/cm^2 on the average and the nuclear heating is 12 W/cm^3. Assuming heat flux of 30 W/cm^2 and nuclear heating of 12 W/cm^3, the transient behavior of the temperature distribution of cooling tube and protection wall has been analyzed by two-dimensional calculations. Cooling tube configuration and analytical conditions used are shown in Fig. 2.2.2. Temperature changes after start up are shown in Figs. 2.2.3-2.2.5. Temperature distributions in the cooling tube and protection wall are shown in Fig. 2.2.6.
of the tube and without it. The stress analysis is described in Section 2.2.2.

The temperature distribution becomes more uniform by the addition of the copper liner. But the integrity of the liner must be demonstrated experimentally. A disign accomodating the heat flux of 30 W/cm^2 is feasible but the fabrication of practicable panel is not easy. The design of cooling

panel will be eased in case of the divertor concept owing to the reduced heat flux.

2.2.2 Stress Analysis of Cooling Tube

The stress analysis of the cooling tube with a copper liner on the inside surface was carried out under internal pressure and temperature distribution shown in Fig. 2.2.6.

Two-dimensional finite elements of plane strain and plane stress conditions were employed for the elastic and thermal stress analysis. The thickness and outside radius of the cooling tube are 2.0 mm and 10.0 mm, respectively.

Fig. 2.2.7 shows the shape of the deformation and the displacements of the cooling tube for the two conditions.

Fig. 2.2.8 shows the distribution of the stress intensity in the plane strain condition and Fig. 2.2.9 shows in the plane stress condition.

The results obtained from this stress analysis shows that the thermal stress depending upon the temperature difference between the side with fin and without fin results from only the stress of the longitudinal direction. The large thermal stress of the direction generated in the area of the fin will reduce if the several cuts are given in the longitudinal direction of the fin. The reasonable deformation and stress of the cooling tube will be present between the results of plane strain and plane stress conditions. In future, it is necessary to carry out a detailed stress analysis with three-dimensional model.

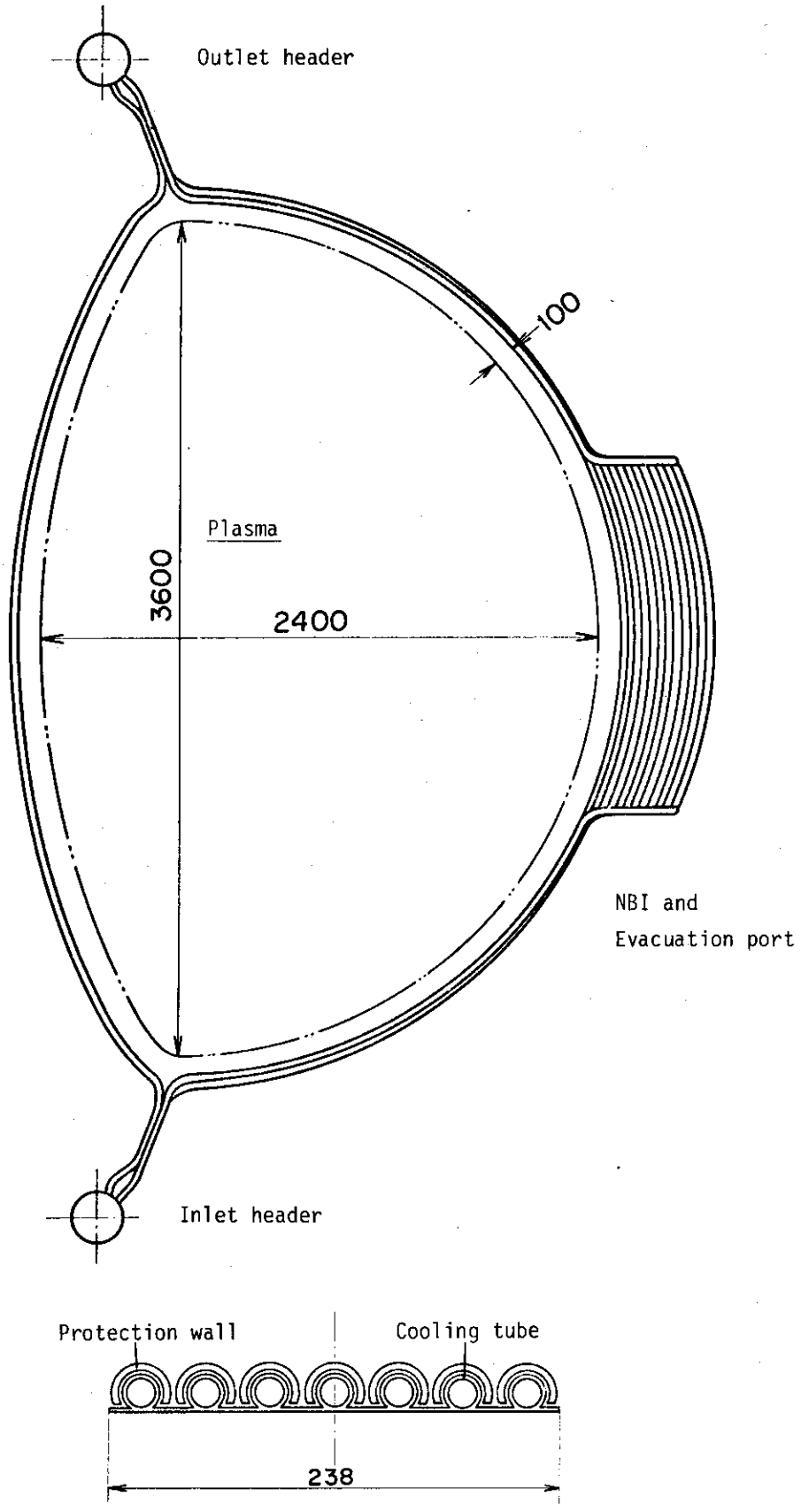

Fig.2.2.1 A conceptual structure of cooling panel

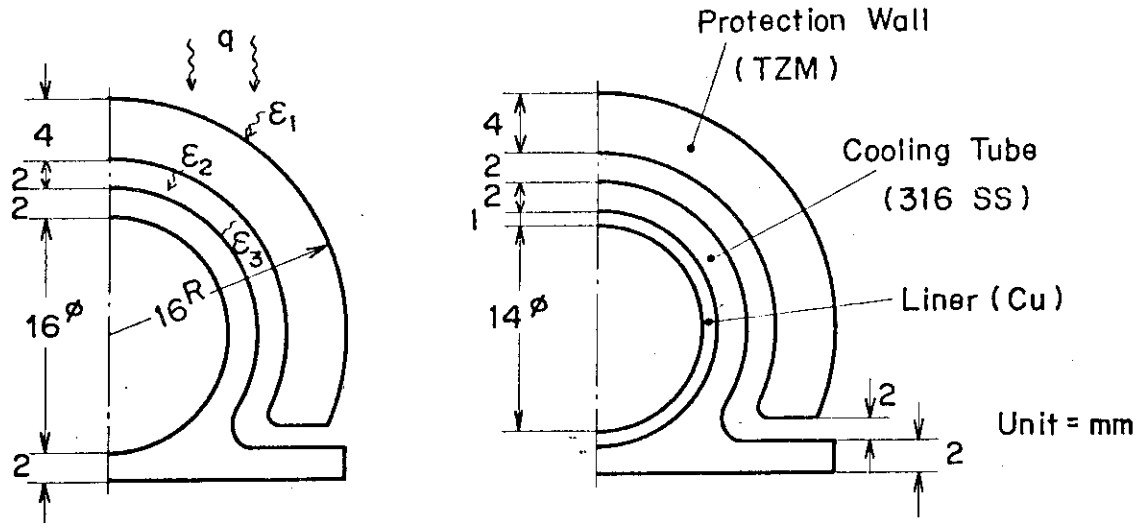

Type A

Type B

q = 30W/cm^2 (Burn Time)
Q = 12W/cc (Burn Time)
ε_1 = 0.4
ε_2 = 0.7
ε_3 = 0.7
k_{TZM} = 0.34-9.09x10^{-5} t
k_{316SS} = 0.046 cal/cms °C
k_{Cu} = 0.8 cal/cms °C

Cp_{TZM} = 0.068 cal/g °C
Cp_{316SS} = 0.13 cal/g °C
Cp_{Cu} = 0.8 cal/g°C
p_{TZM} = 10.2g/cc
p_{316SS} = 8.0g/cc
p_{Cu} = 8.96g/cc

h = 0.130 cal/cm^2 s °C
He Temp. = 300°C

Fig. 2.2.2 Cooling tube configulations and analytical conditions

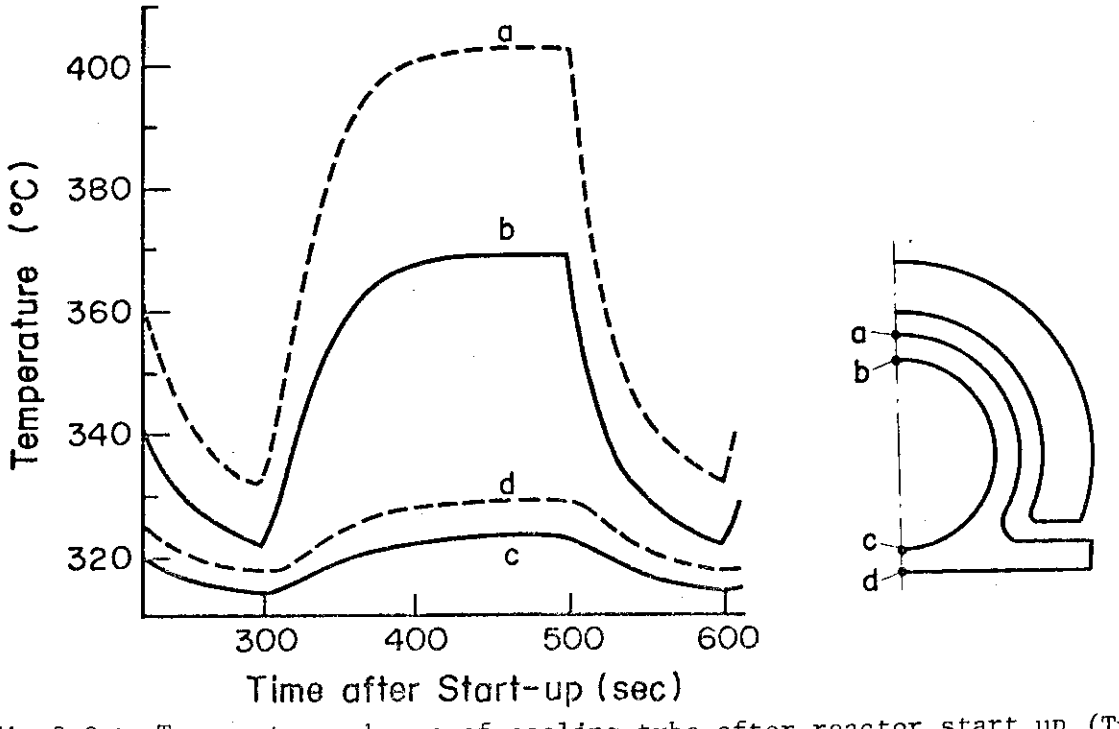

Fig.2.2.3 Temperature change of cooling tube after reactor start up (Type A)

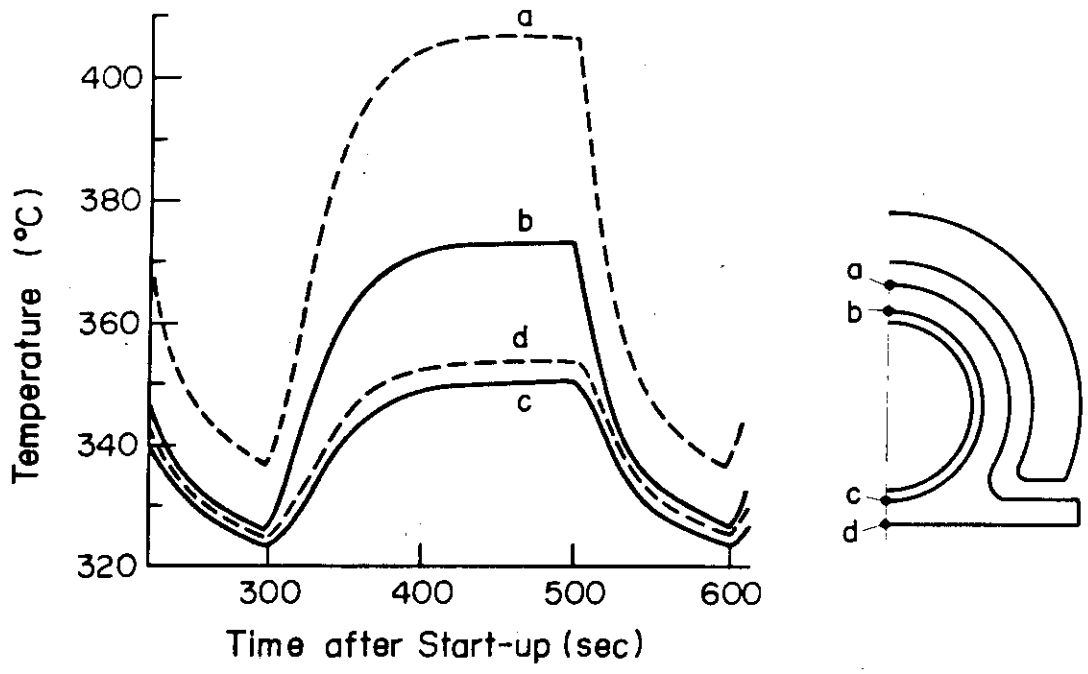

Fig.2.2.4 Temperature change of cooling tube after reactor start up (Type B)

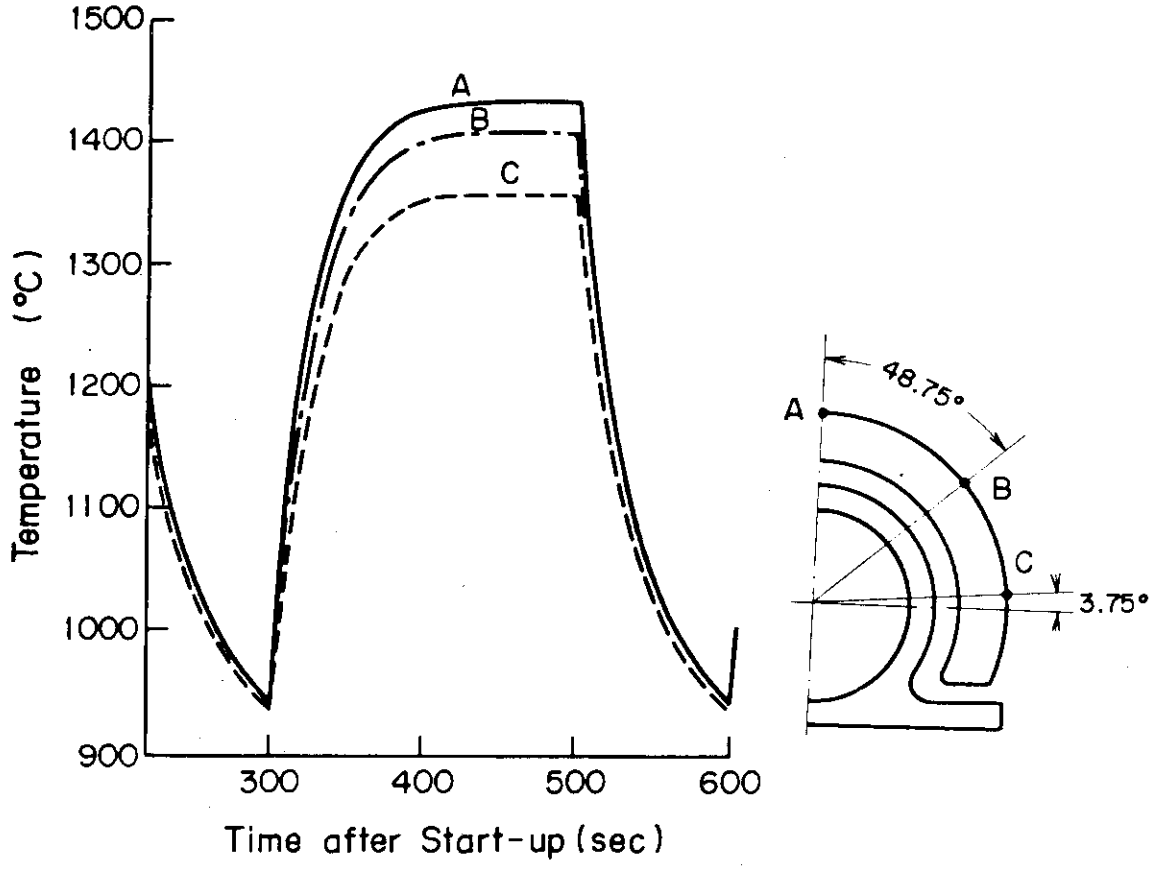

Fig.2.2.5 Temperature change of protection wall after reactor start up

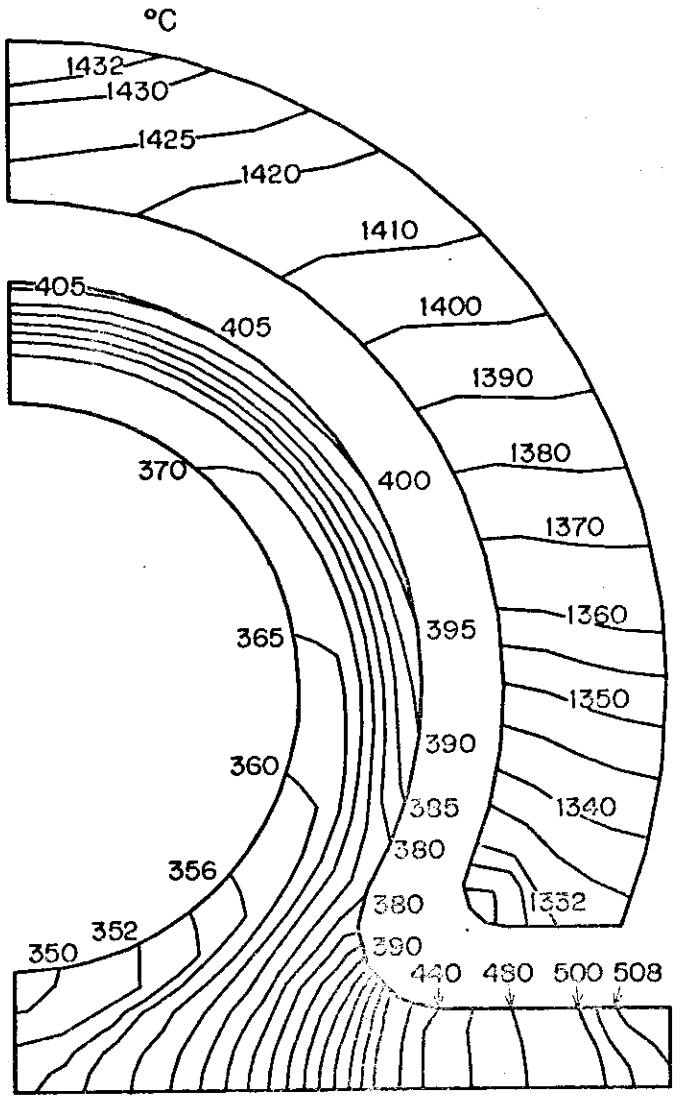

Fig.2.2.6 Temperature distribution in the cooling tube and protection wall (Type-B)

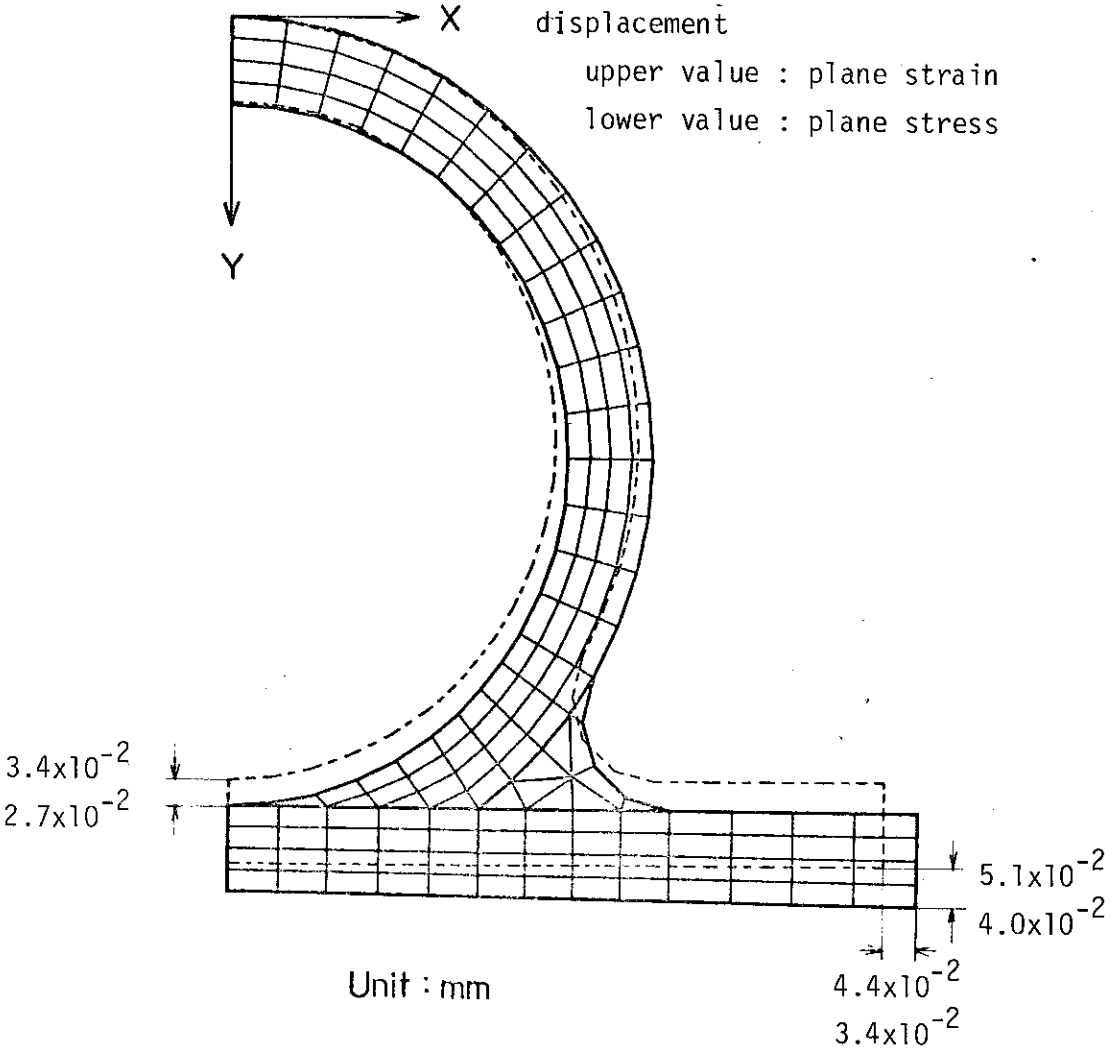

Fig.2.2.7 The shape of the deformation and the displacements of the cooling tube for two conditions

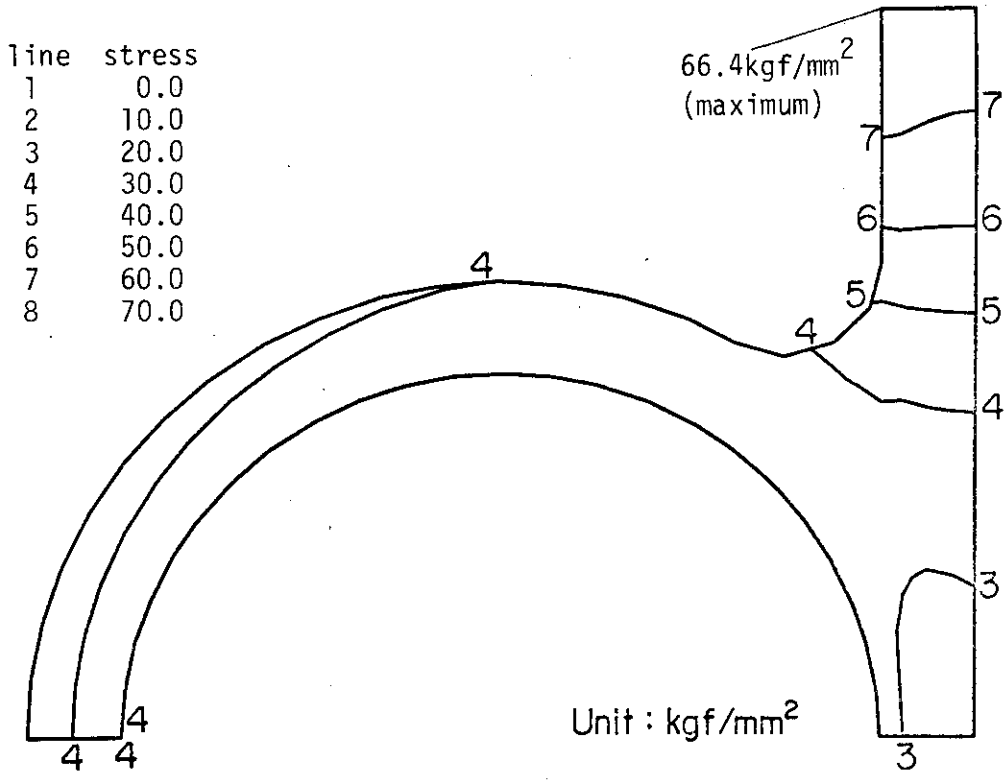

Fig.2.2.8 The distribution of the stress intensity for plane strain condition

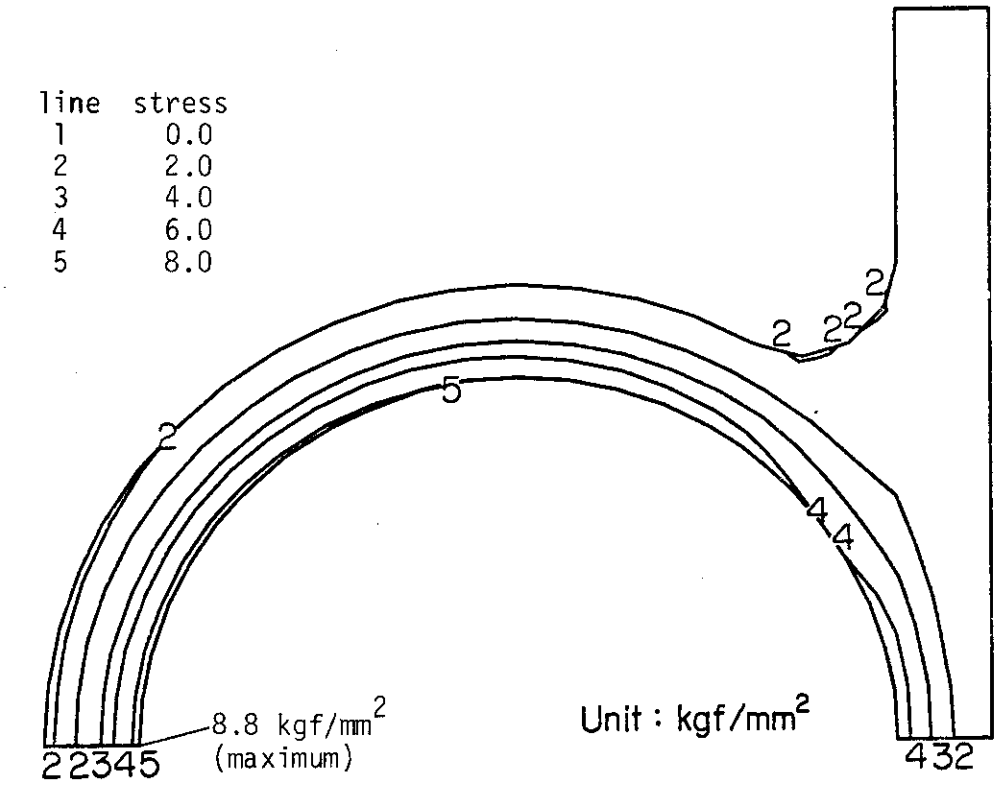

Fig.2.2.9 The distribution of the stress intensity for plane stress condition

2.3 Primary Shield (Vacuum Chamber)

Requirements for a vacuum chamber is to keep the inside of the chamber at a high vacuum and to increase the one-turn resistance. Further in view of the evacuation the surface area of the chamber should be reduced as small as possible. The choice of the location of the chamber is important to meet these requirements.

We placed the vacuum vessel on the inner side of the bulk shield for the following reasons.

i) Locating the vacuum chamber further outward causes a difficulty in evacuation.

ii) The outside of the blanket is too complicated to obtain a vacuum-tight structure.

iii) Placing the vacuum chamber near a plasma is very difficult to design in view of large nuclear heating and a serious problem of electromagnetic force.

Further in cases of ii) and iii) the repair is very difficult.

Major radius and inner bore are 5.0 m, 4.4m x 6.8m, respectively. From the consideration of the spatial arrangement, the thickness of the shielding is determined to be 0.4 m at the smaller radius part, and 1.0 m at the larger radius part. The shielding structure is divided into 6 sectors along the torus for assembling and disassembling the reactor. One NBI port is attached to the outer radius part of the one-sixth shielding.

The main structure of the shielding is formed by the stainless steel panels and is filled up with tungsten alloy and other shielding materials. About 10 v% of water channels are provided on stainless steel panels to remove the nuclear heating.

To form the vacuum barrier, stainless steel lining is fixed to the inside (blanket side) of the shielding structure. Some part of the lining consists of bellows to acquire high electrical resistivity (more than 0.2 mΩ) along the torus. Seal welding between the flanges of each two neighboring one-sixth sectors is employed for vacuum enclosure. The vacuum lining except the bellows is cooled by water to remove the thermal radiation heat from the blanket. The bellows are protected from the thermal radiation by the aluminum alloy plate. At the outside of the stainless steel-tungsten alloy structure, lead layer is fixed for gamma-shielding. But at the smaller major radius part, this lead layer is excluded for spatial arrangement requirement.

2.4 Divertor Plate

The heat flux flowing to the divertor plate is estimated to be 40～50 MW[1]. For the divertor plate having the structure shown in Figure 1.3, the peak heat flux is expected to be 200 W/cm^2 and the average to be 100 W/cm^2. In this case the ion flow is swung by changing the divertor-coil current in a sine wave mode.

Assuming copper tubes as the divertor plate and a frequency of 1 Hz, the transient behavior of the plate temperature has been analyzed by two-dimentional calculations. Analytical conditions are shown in Table 2.4.1 and the results are shown in Fig. 2.4.1-5. These calculations are performed with circular tube of Cu for rough estimation. It seems that we could handle such a degree of heat load. However, there are many problems left, such as radiation damage, thermal cycle fatigue, fabrication and repairable structure, which need further investigations.

Reference

1) Y. Shimomura, K. Sako, K. Shinya : "Some Considerations of Ash Enrichment and Ash Exhaust by a Simple Divertor", JAERI-M 8294 (1979).

Table 2.4.1 Analytical conditions

Heat flux on the plate

$q = q_o \sin \pi t$, t = sec , q_o = 200W/cm^2

Heat flux on the tube surface

$q_\theta = q_o \cos\theta \cdot \sin \pi t$

Tube size case 1 Outer dia.= 20mm
Inner dia.= 10mm
case 2 Outer dia.= 30mm
Inner dia.= 10mm

Coolant He , 100°C , 100ata , 100m/sec
H_2O , 10ata (Saturation Temp.= 179°C)

Heat transfer coefficient

He : 0.33cal/cm^{2}s°C
H_2O : $1.16 \times 10^{-4} (\Delta t)^3$ cal/cm^{2}s°C

Thermal properties of Cu

k : 0.8cal/cms°C
ρ : 8.96g/cc
C_p : 0.092cal/g°C

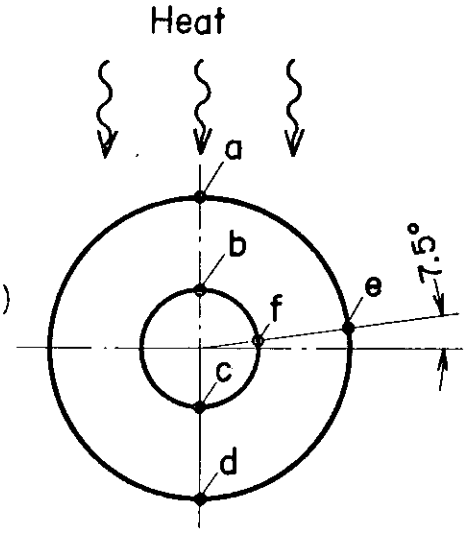

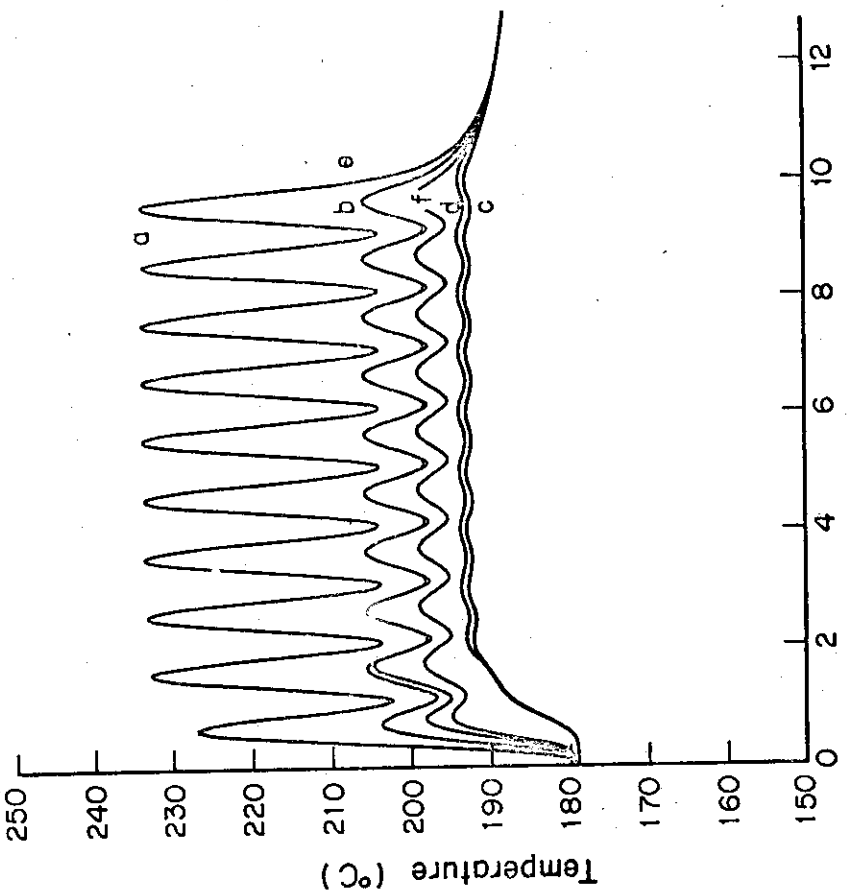

Fig. 2.4.2 Transient behaviour of the tube temperature (Case 1, H_2O)

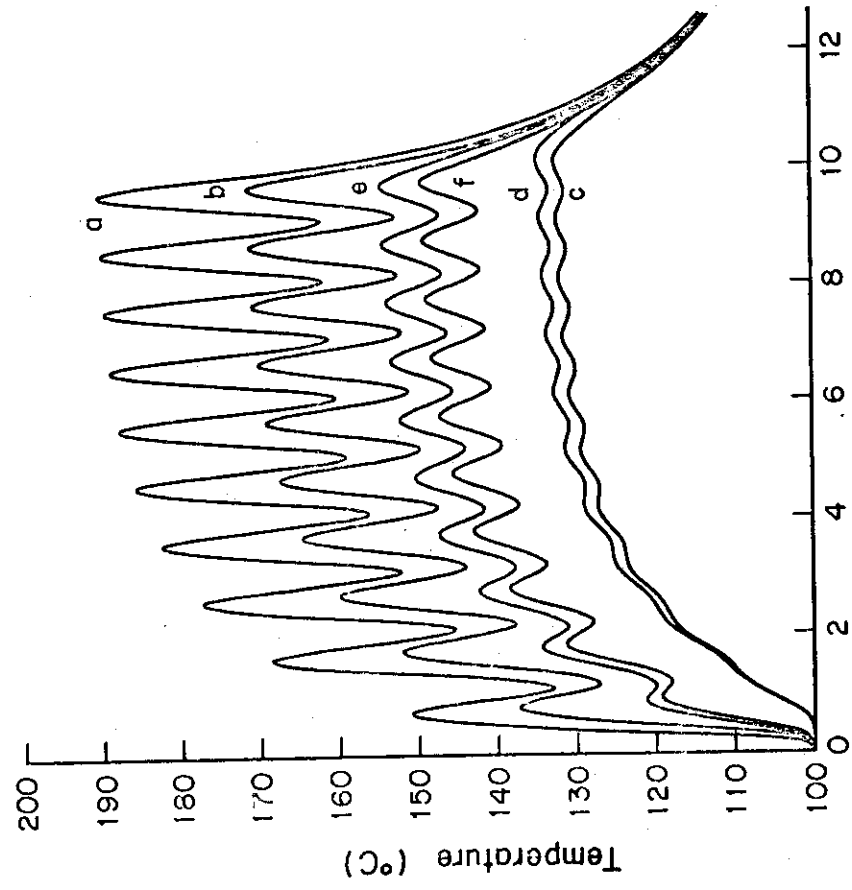

Fig. 2.4.1 Transient behaviour of the tube temperature (Case 1, He)

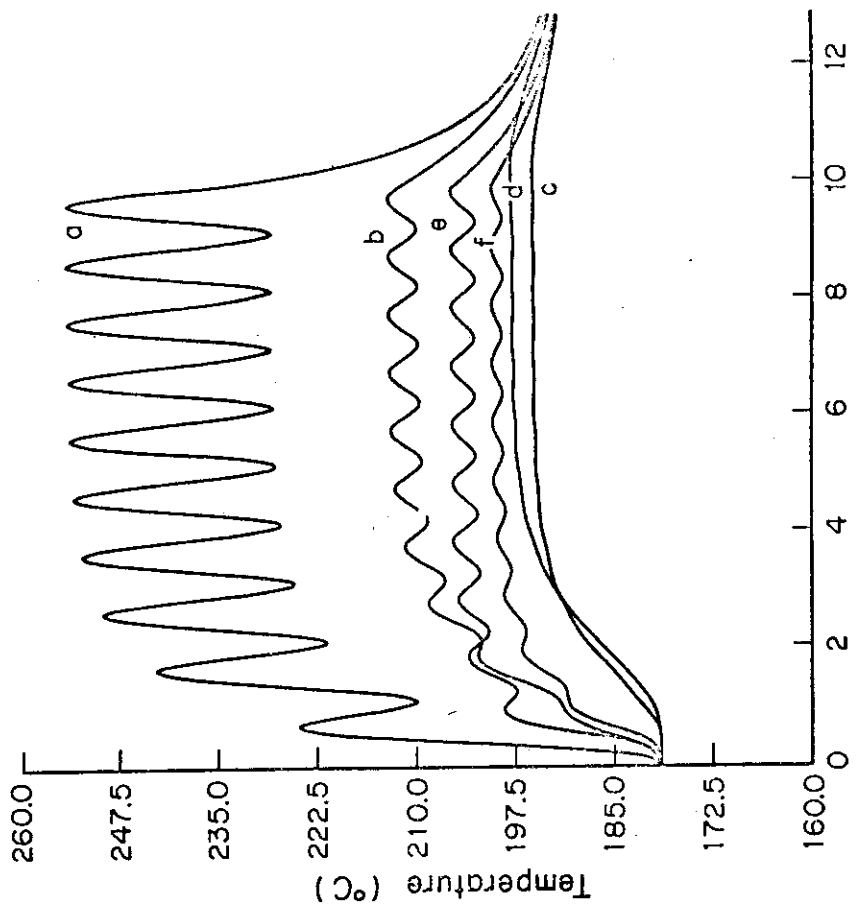

Fig. 2.4.4 Transient behaviour of the tube temperature (Case 2, H_2O)

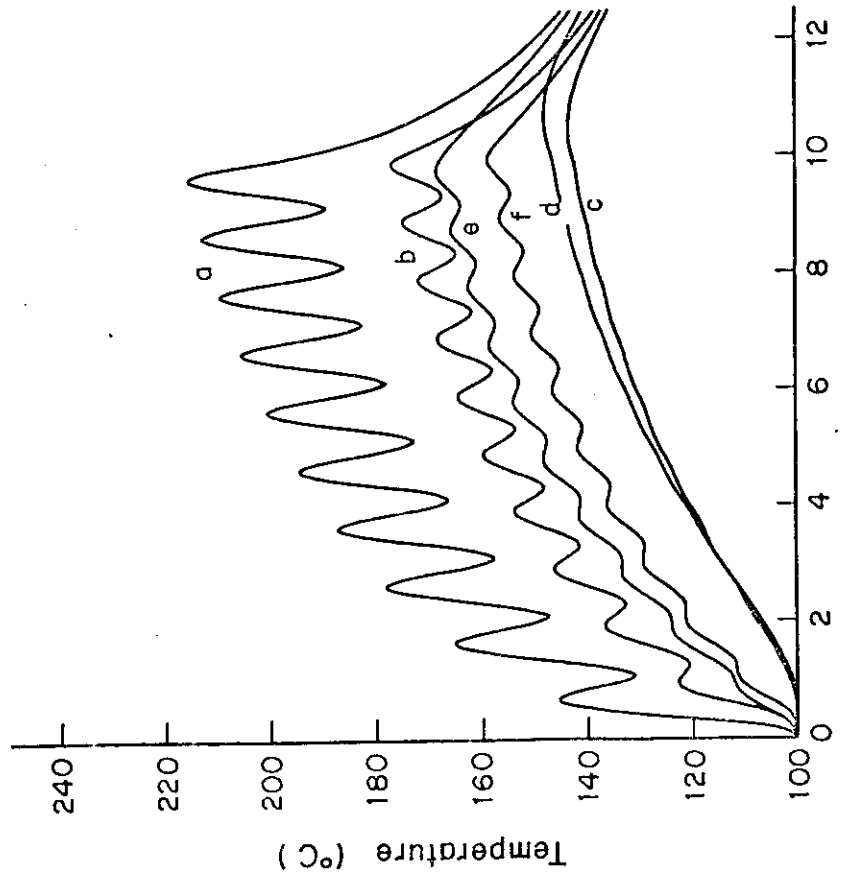

Fig. 2.4.3 Transient behaviour of the tube temperature (Case 2, He)

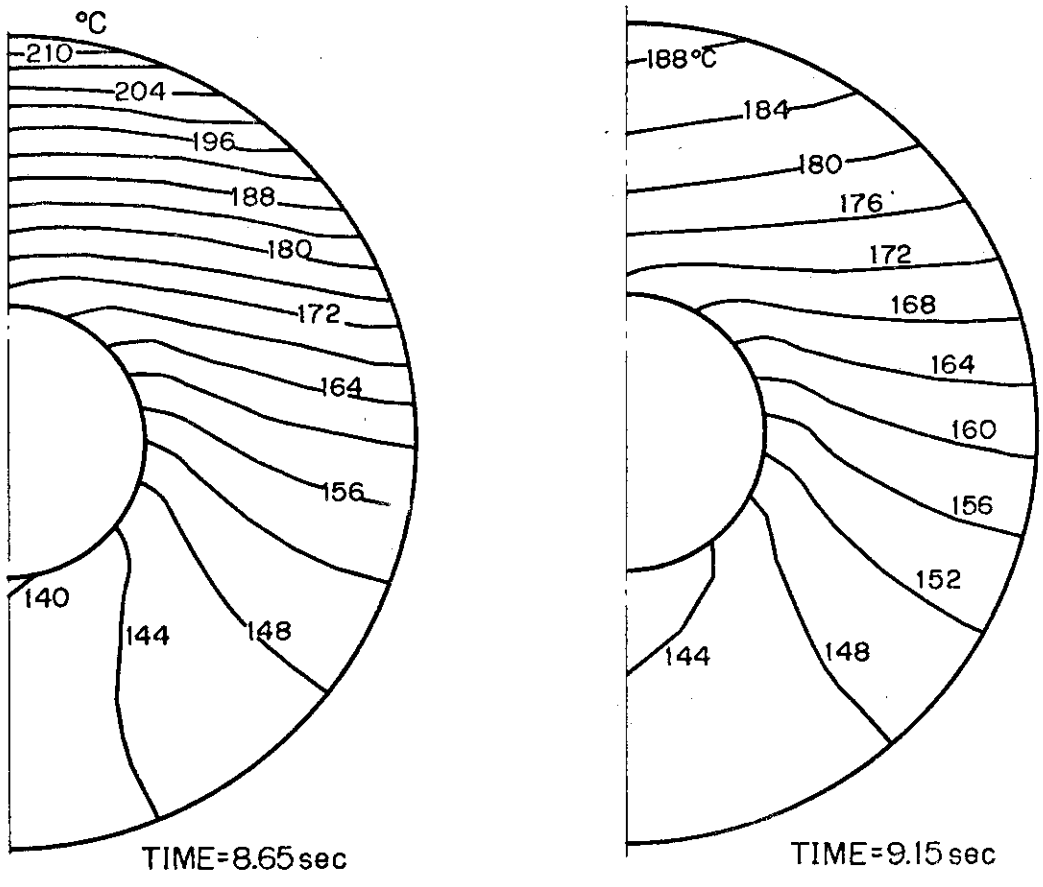

Fig. 2.4.5 An example of temperature distribution in the tube (Case 2, He)

3. Blanket Neutronics and Shielding

3.1 Tritium breeding ratio

To estimate tritium breeding ratio of INTOR blanket mentioned above, three cases of calculation are carried out.

Figure 3.1 shows the calculational model of case 1 which is performed by using one-dimensional Sn transport code ANISN. Figure 3.2 shows the triton production distribution obtained by this code. The case 2 and case 3 are three-dimensional calculations by Monte Carlo transport code MORSE-I. Figure 3.3 shows the calculation model of the case 2. In this case, torus geometry of plasma, blanket and shield, neutron source density distribution and the difference between the compositions of inner and outer blankets are taken into account while in one-dimensional calculation they are not. The case 3 is a three-dimensional blanket cell model which takes account of heterogeneity of the cell. Figures 3.4 and 3.5 show the calculational model of the case 3. Table 3.1 shows tritium breeding ratios estimated in the three cases. The case 1 and the case 3 give almost same value of tritium breeding ratio, so the effect of blanket cell heterogeneity must be very small in this case. The tritium breeding ratio for the case 2 is about two thirds of that for the case 1. It is because the case 2 takes account of the fact that the inner blanket does not contain breeding materials. It is almost impossible to load breeding materials in the inner blanket of a small-sized tokamak reactor such as INTOR because the inner blanket is required to be a high energy neutron shield rather than tritium breeding blanket. The tritium breeding ratio of INTOR with blanket cells as shown in Figure 2.1.2 is estimated to be about 0.6 according to the case 2 calculation.

Table 3.1

	Tritium Breeding Ratio		
	^{7}Li	^{6}Li	Total
Case 1	0.157	0.751	0.908
Case 2	0.127	0.487	0.614
Case 3	0.158	0.734	0.892

The power density distribution is obtained by the following process. In the MHD equilibrium, pressure is expressed by the flux function Ψ as follows :

$$P = P_0 \psi^{\zeta}$$

Here, ion temperature and density distribution can be assumed as follows :

$$T = T_0 \psi^{\eta}$$

$$n = n_0 \psi^{\xi}$$

$$\eta + \xi = \zeta$$

For the MHD equilibria of INTOR, the value of ζ is 1.48, so η =1.0 is assumed for this calculation.

The power density distribution for the ion temperature, and density distribution which give the $\bar{T}$= 10 KeV is shown in figure 3.6 .
Here, $\bar{T}$ is defined as

$$\bar{T} = \frac{\int nT \, dv}{\int n \, dv}$$

and the fusion reaction cross section used in this calculation is

$$\langle \sigma v \rangle = 370.0 \exp(-20.x \, Ti^{-\frac{1}{3}}) \; / \; ((1+ (Ti/70)^{1.3}) \times Ti^{\frac{2}{3}})$$

Reference

1) Horton, W. Jr. and Kammash, T. Nuclear Fusion 13, (1973) 753

3.2 Nuclear Heating

Removal of nuclear heating in the first wall is a severe problem for blanket structural design when a neutron wall loading is large. In INTOR case the nuclear heating might be a severe problem. So, as well as tritium breeding ratio, nuclear heating densities are also calculated for the three cases previously mentioned.

Figure 3.7 shows the poloidal distributions of nuclear heating density in the first wall (case 2). The peaking factor is estimated to be 1.25 ~ 1.3 according to this figure. However, it should be noted that the average nuclear heating density in the first wall of a three dimensional calculation is not always equal to that of a one-dimensional calculation. Actually, the average nuclear heating in the case 2 is 7.6 w/cc while that in the case 1 is 10 w/cc. It is partly because of the difference between fusion power density distributions assumed in one-dimensional and three-dimensional calculation. In the case 1, uniform fusion power density distribution is assumed while in the case 2 the distribution shown in Figure 3.6 is assumed.

Figure 3.8 shows the calculational result of the case 3. For calculation of thermal stress of blanket vessel this nuclear heating density distribution will be used.

3.3 Bulk shielding

As the first step of the shielding design for the INTOR proposal, one-dimensional bulk shielding calculations are carried out. An optimization study of the shield material on the inside of the torus was performed to minimize the displacement damage of the copper stabilizer of the super-conducting toroidal field magnet. On the other hand, the thickness and the constituent materials of the blanket on the outside of the torus were determined mostly from the requirements for tritium breeding and from the results of a thermal and structural analysis. The outer shield configuration was determined by the criteria of allowing personnel access to the outside of the shield.

Cylindrical calculational models for the inner and outer shield are given in Tables 3.2 and 3.3, respectively. Table 3.4 summarizes the tentative criteria and the results obtained from one-dimensional shielding calculations for the inner and outer super-conducting magnets (SCM) of the INTOR proposal. Cumulative fluence are calculated assuming 25% availability and 10 years lifetime. Copper is supposed to be annealed to room temperature

once every year.

Figures 3.9 and 3.10 show the neutron and gamma-ray fluxes for the inner and outer models, respectively. Nuclear heating rates in the inner and outer models are depicted in Figs. 3.11 and 3.12. Cumulative dose rate in epoxy over 10 years lifetime in the inner and outer models are shown in Figs. 3.13 and 3.14, respectively.

As shown in Table 3.4, the inner model of Table 3.2 with the total bulk thickness of 71.5 cm satisfies all of the tentative criteria adopted for the SCM irradiation by a factor of two. This means the total shield thickness can be reduced a few centimeters if the present criteria proves to be reliable. But with the estimated error of the calculated result being $\sim$100%, there is little sense in the reduction.

The minimum thickness of 71.5 cm is obtained under several limitations based on a thermal and structural analysis. By choosing the shield material considering only the shielding effectiveness, the shield thickness may be reduced another ten centimeters under the same tentative shielding requirement criteria. However 71.5 cm seems to be a practical limit for a realistic design.

Table 3.2 Inner model for the INTOR proposal

Region No., i	Region	Region Radius, r_i(cm)	Mesh No., j_i	$\sum_i j_i$	Mesh Width Δr_i(cm)
1.	Plasma	120.0	1	1	120.0
	Vacuum	133.5	1	2	13.5
2.	TZM protection wall	134.5	2	4	0.5
3.	SS tube wall	135.0	2	6	0.25
4.	SS(80%) + H_2O(20%)	145.0	5	11	2.0
5.	SS(90%) + H_2O(10%)	165.0	10	21	2.0
6.	Vacuum	170.0	1	22	5.0
7.	SS(30%) + W(40%) + Borated water	210.0	40	62	1.0
8.	Air	220.0	1	63	10.0
9.	SS cryostat vessel	225.0	2	65	2.5
10.	SCM, SS(60%) + Cu(28%) + Nb(7%)	310.0	40	105	2.125

Table 3.3 Outer model for the INTOR proposal

Region No., i	Region	Region Radius, r_i(cm)	Mesh No., j_i	$\sum_i j_i$	Mesh Width Δr_i(cm)
1.	Plasma	120.0	1	1	120
	Vacuum	133.5	1	2	13.5
2.	TZM protection wall	134.5	2	4	0.5
3.	SS tube + cell wall	137.0	2	6	1.25
4.	Li_2O(21.3%) + SS(4.74%) + He(21.3%)	155.0	6	12	3.0
5.	Li_2O(53.05%) + SS(20.15%) + He(10.5%)	181.6	16	28	1.66
6.	SS end wall	185.0	2	30	1.7
7.	Vacuum	270.0	1	31	85.0
8.	SS(90%) + Borated water(10%)	370.0	50	81	2.0
9.	Air	380.0	1	82	10.0
10.	SS cryostat vessel	385.0	2	84	2.5
11.	SCM, SS(60%) + Cu(28%) + Nb(7%)	480.0	40	124	2.375

Table 3.4 Results of bulk shielding design calculations of superconducting magnets for the INTOR proposal

Items*)	Tentative design criteria	Values at inner SCM	Values at outer SCM**)
Maximum DPA in copper (DPA/year)	9.8×10^{-5}	4.3×10^{-5}	4.7×10^{-8}
Maximum neutron fluence (n/cm^2)	2.0×10^{18}	1.1×10^{18}	2.4×10^{15}
Maximum nuclear heating ($Watt/cm^3$)	10^{-3}	1.2×10^{-4}	2.4×10^{-7}
Maximum epoxy dose (rad)	2.4×10^{9}	1.2×10^{9}	1.5×10^{6}

*) Availability and the reactor lifetime are assumed to be 25% and 10 years, respectively.

**) The values at outer SCM surface should be multiplied by ~30 if the effect of neutron streaming through the injection ports are taken into account.

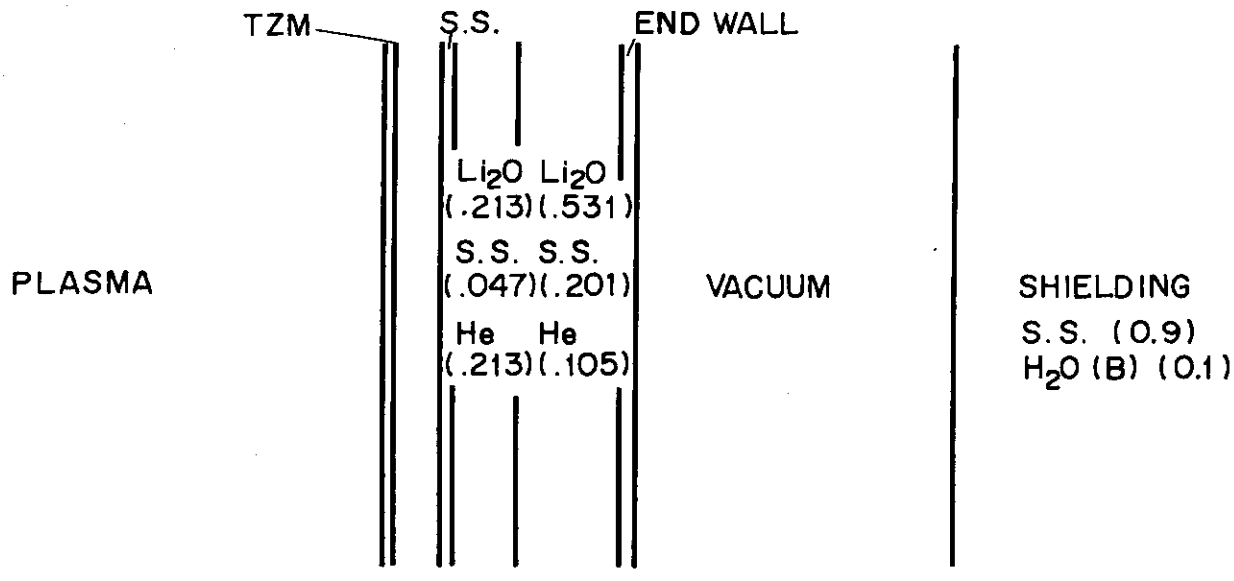

Fig. 3.1 One-dimensional Calculation Model of INTOR-J

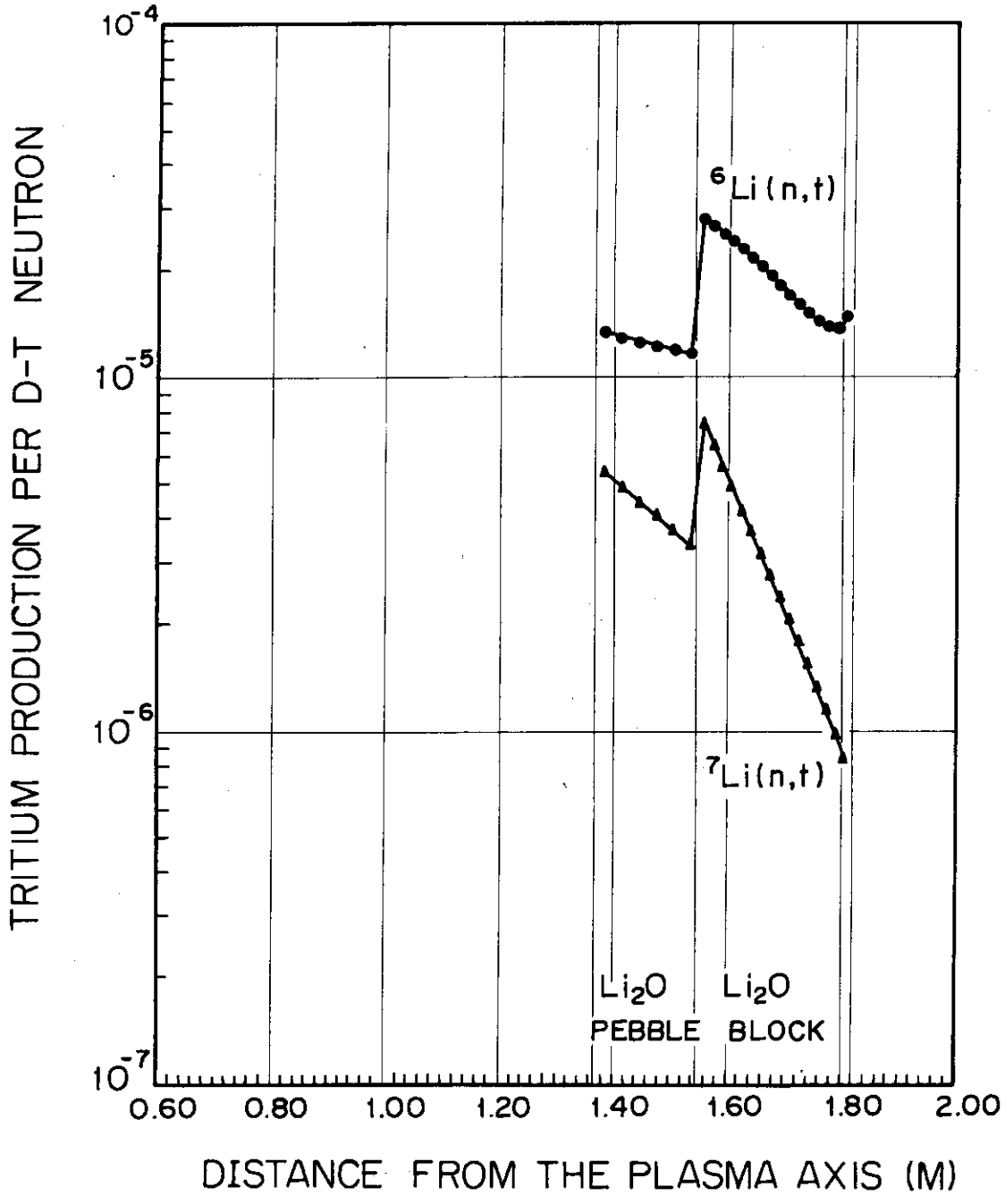

Fig. 3.2 Tritium Production Distribution in Outer Blanket

1 Vacuum
2 Protection wall
3 First wall
4 S.S. (0.8)+H_2O (0.2)
5 S.S. (0.9)+H_2O (0.1)
6 Li_2O (0.213)+S.S.(0.047)
+He (0.213)
7 Li_2O (0.5305)+S.S.(0.2015)
+He (0.105)
8 End wall
9 Inner shield
10 Outer shield

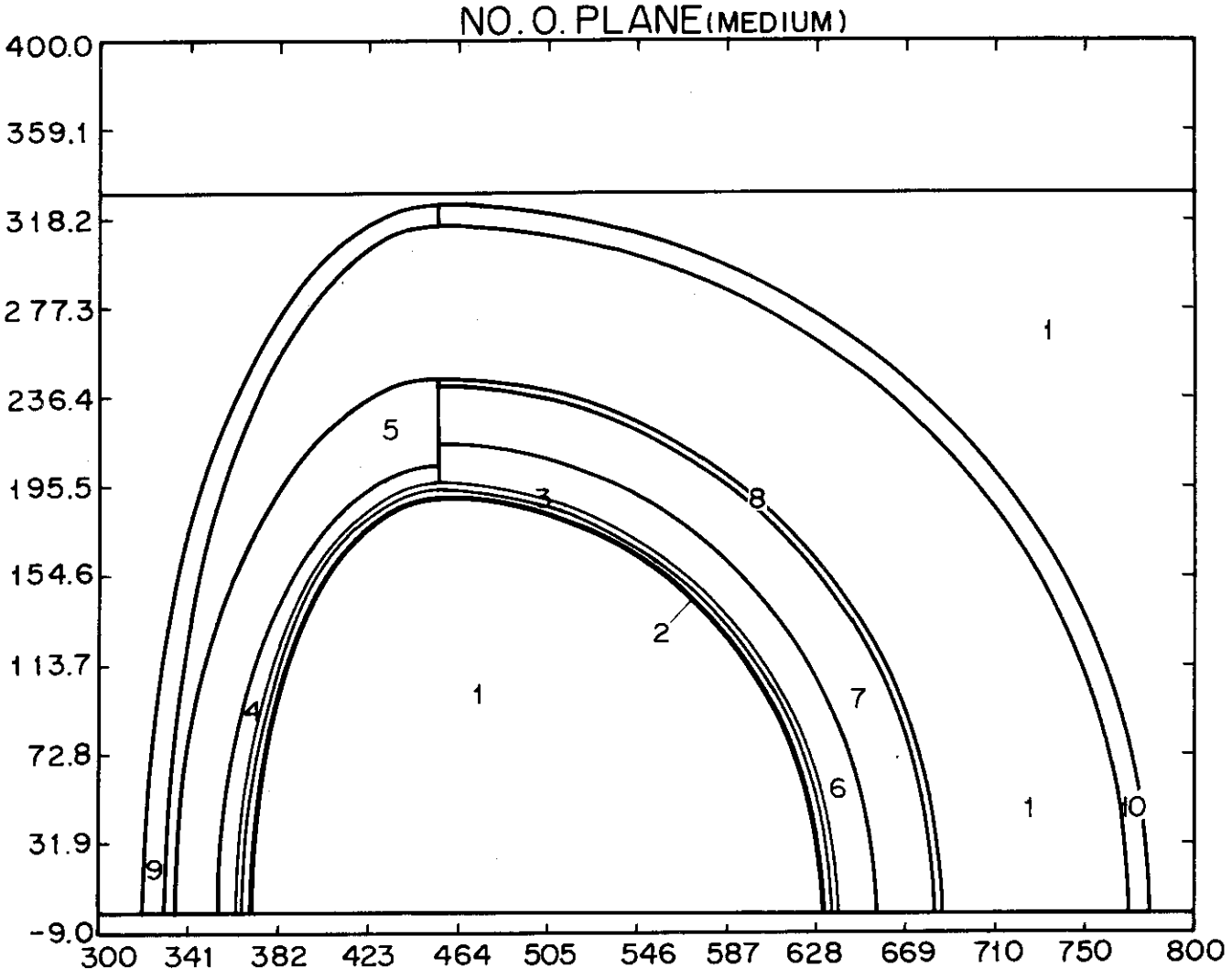

Fig. 3.3 Three-dimensional Calculation Model of INTOR-J

1 Vacuum
2 Protection wall
3 S.S.
4 Li_2O (0.45) + S.S. (0.1)
  He (0.45)
5 Li_2O (0.6697) + S.S. (0.0837)
  He (0.0837)

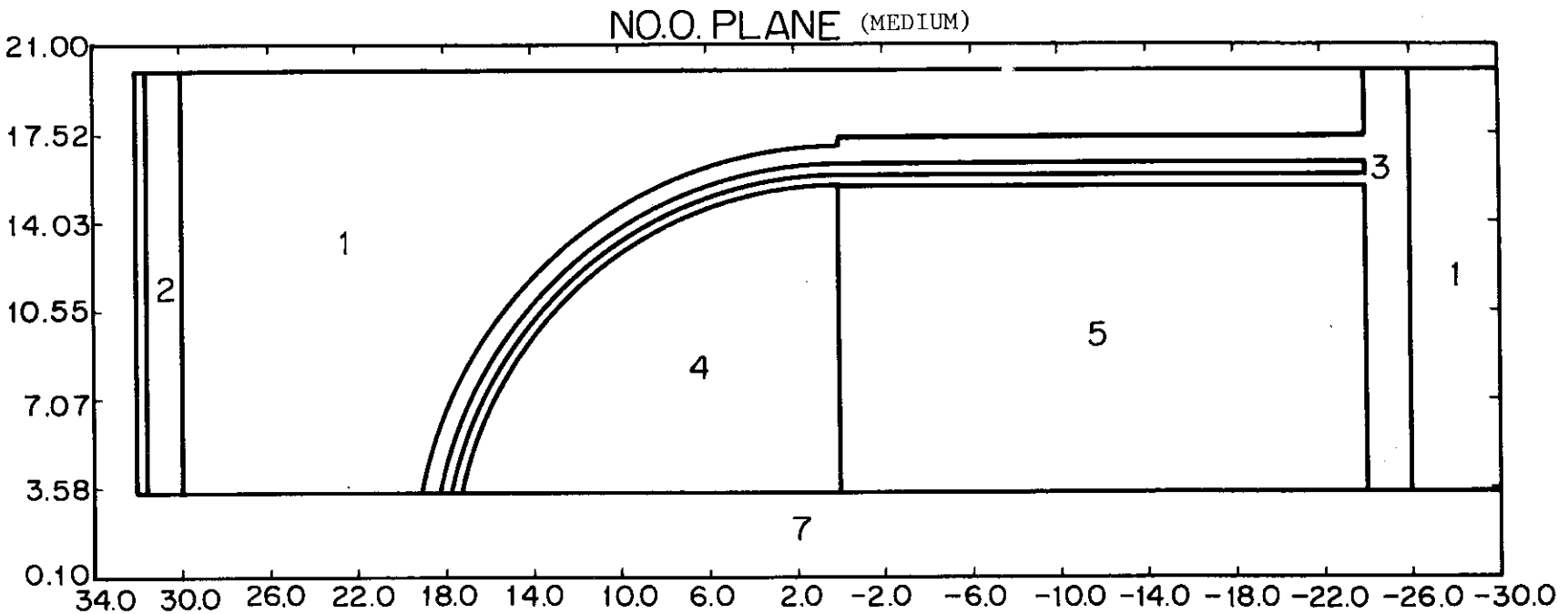

Fig. 3.4 Three-dimensional Calculation Model of Blanket Cell

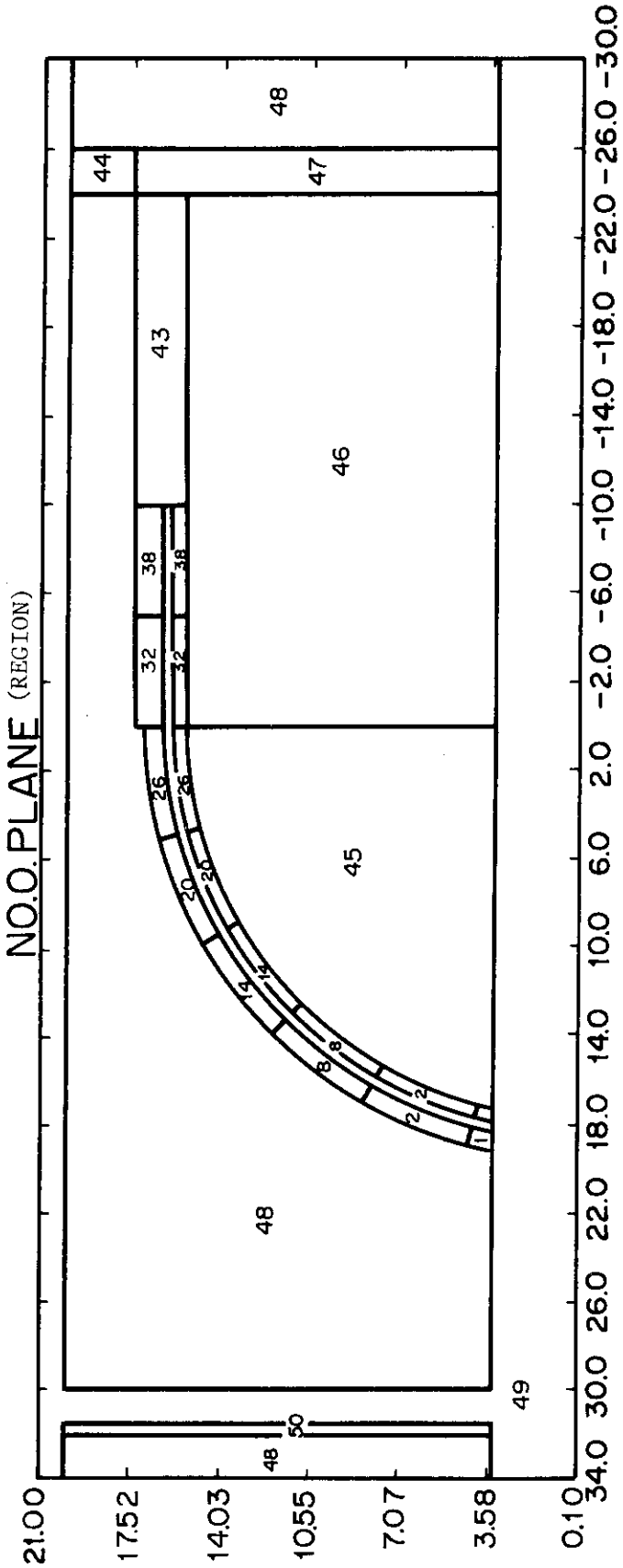

Fig. 3.5 Nuclear Heating Density Editing Region for Blanket Cell

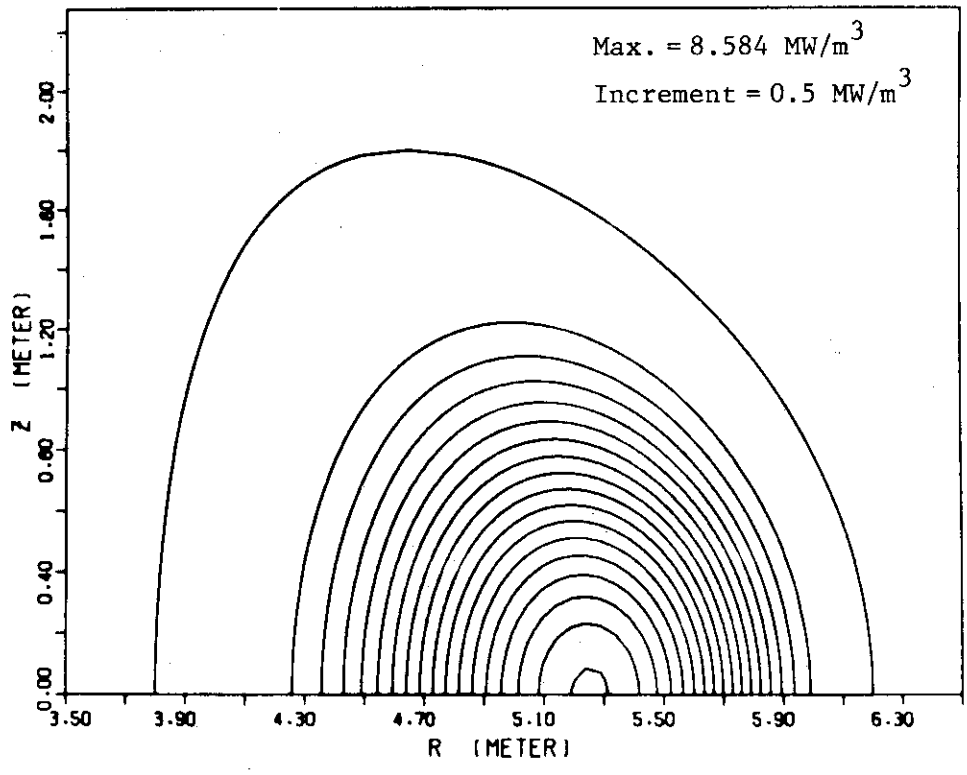

Fig. 3.6 Power density contour

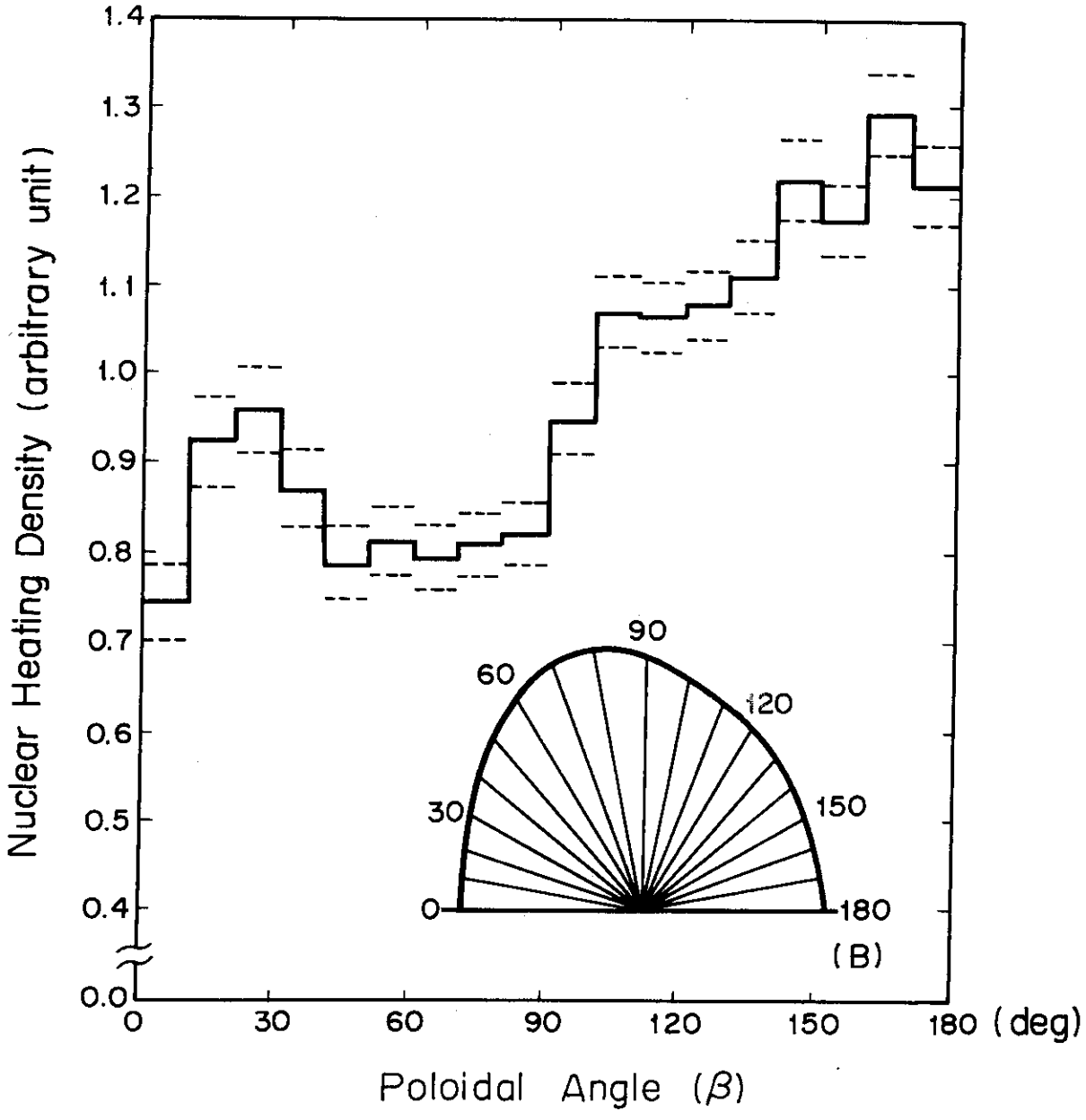

Fig. 3.7 Nuclear Heating Density Distribution in the First Wall

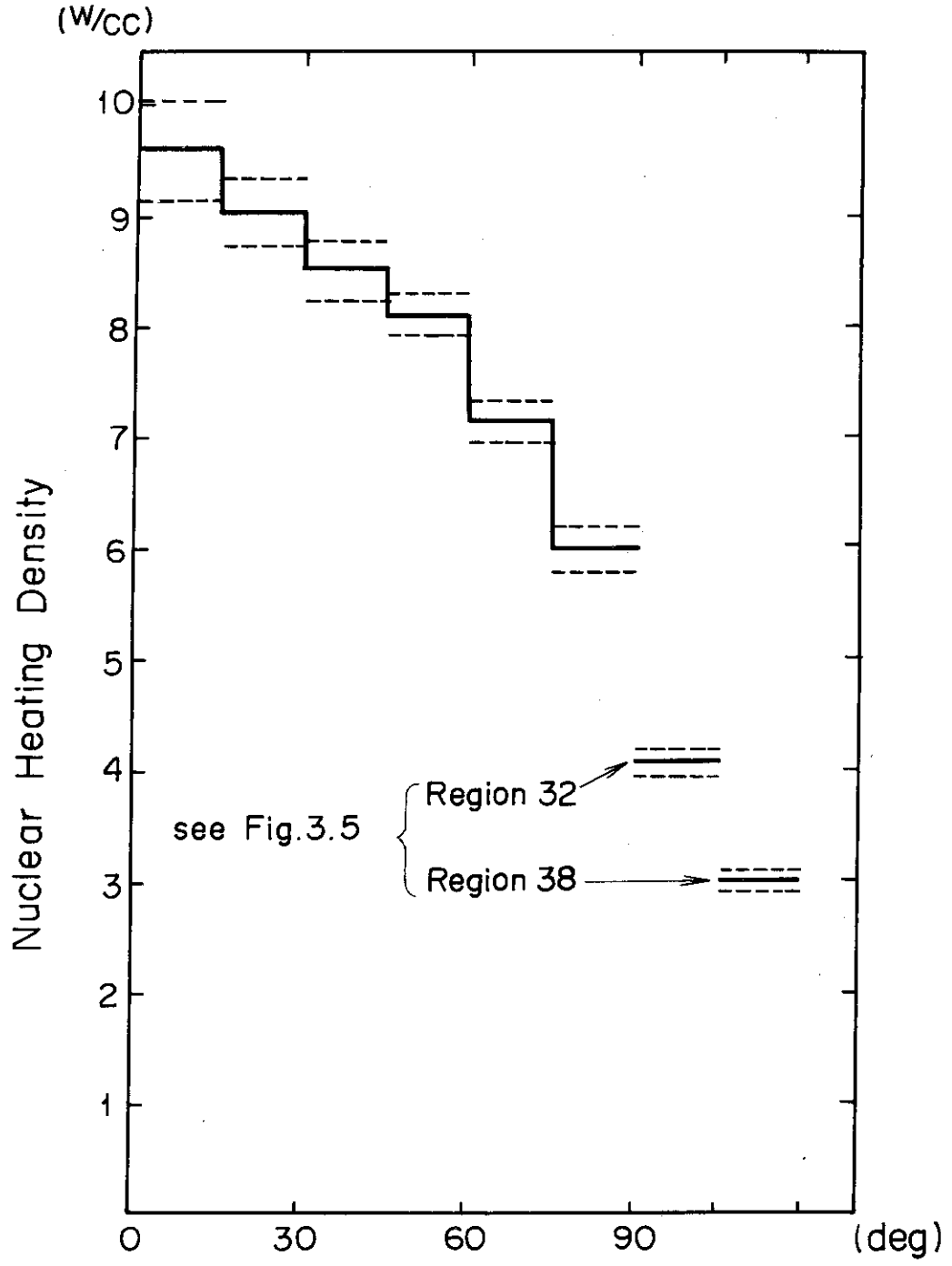

Fig.3.8 Nuclear Heating Density Distribution on the Blanket Dome

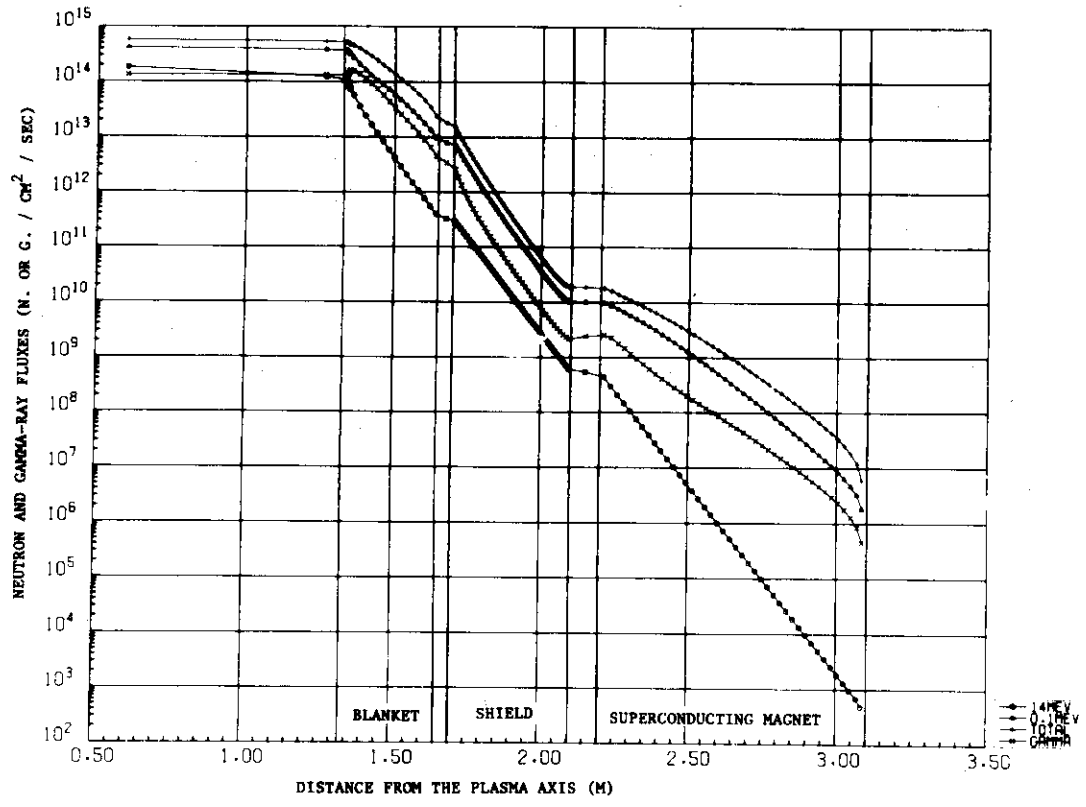

Fig. 3.9 Neutron and gamma-ray fluxes in the inner blanket, shield and toroidal field coil

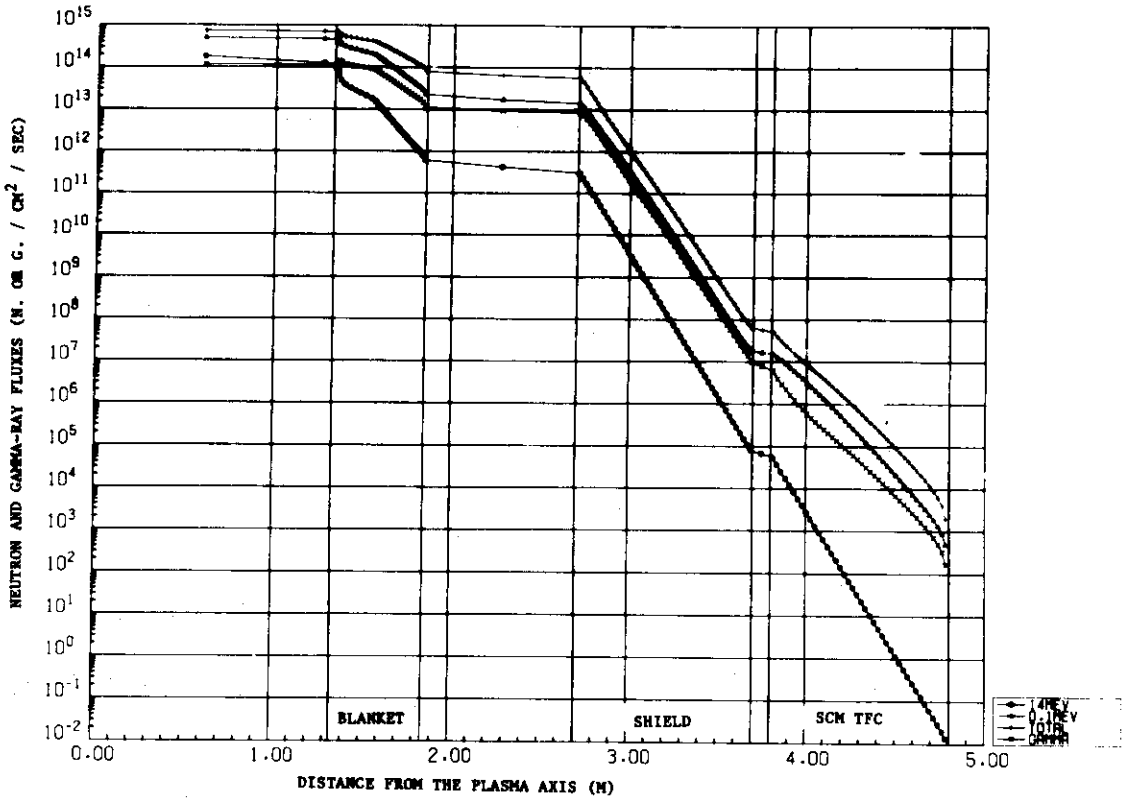

Fig. 3.10 Neutron and gamma-ray fluxes in the outer blanket, shield and toroidal field coil

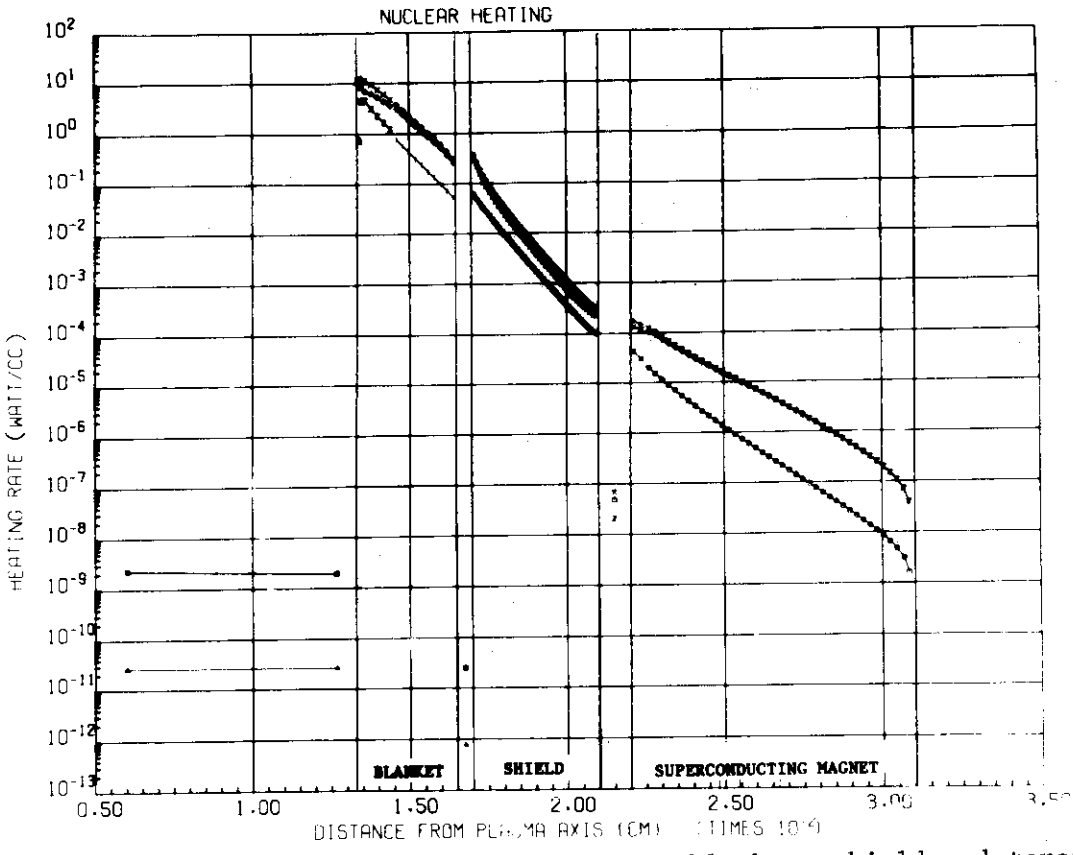

Fig. 3.11 Nuclear heating rate in the inner blanket, shield and toroidal field coil

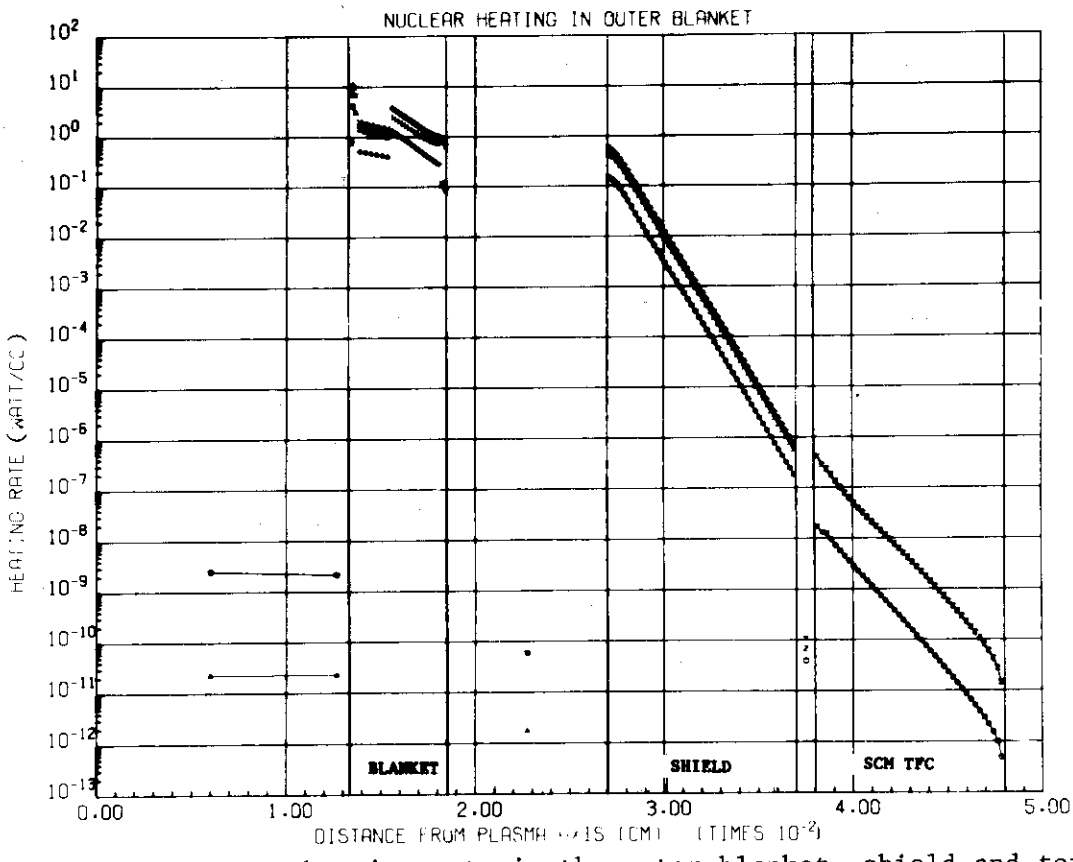

Fig. 3.12 Nuclear heating rate in the outer blanket, shield and toroidal field coil

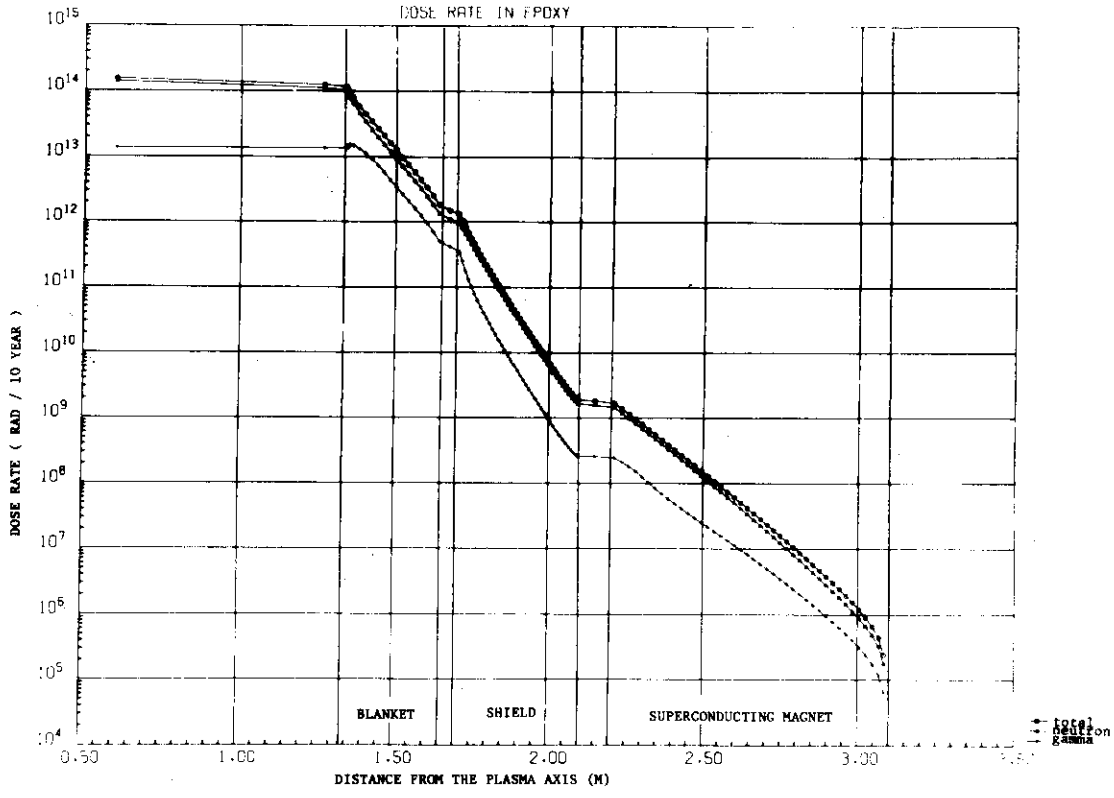

Fig. 3.13 Cumulative epoxy dose rate in the inner blanket, shield and toroidal field coil

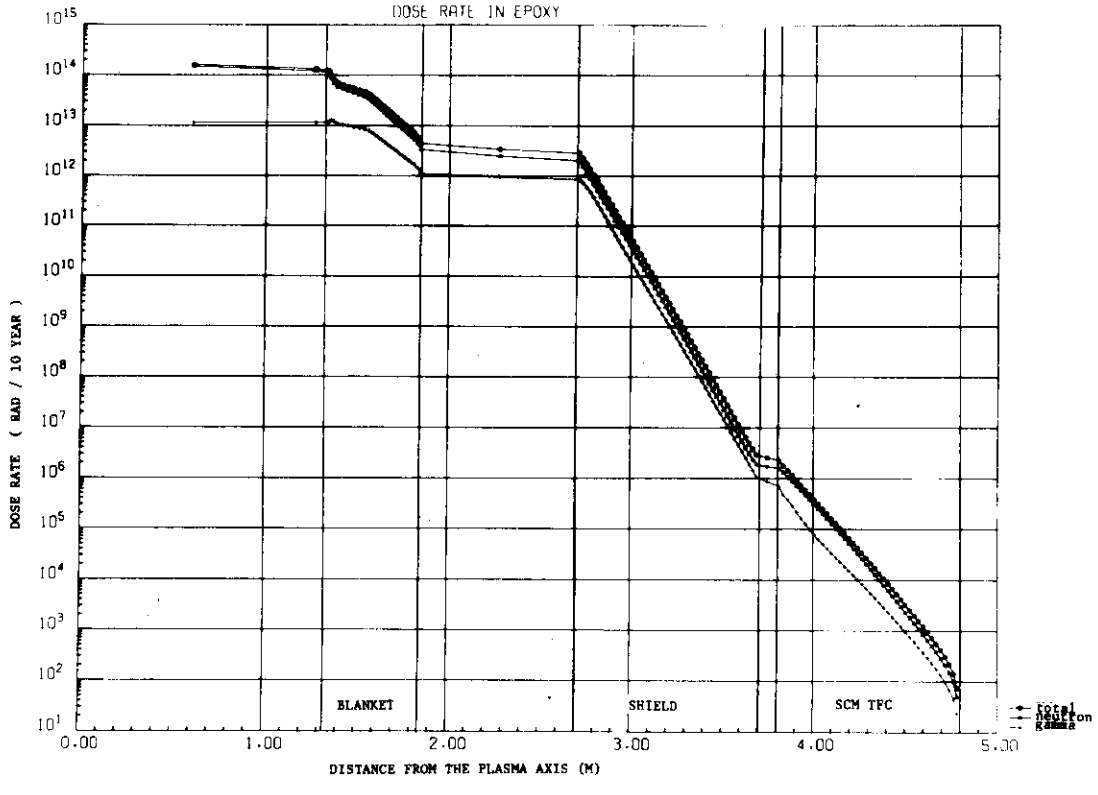

Fig. 3.14 Cumulative epoxy dose rate in the outer blanket, shield and toroidal field coil

4. Superconducting Magnets

4.1 Toroidal Field Magnet

The fundamental design requirements for the toroidal field magnet design are as follows,

(1) toroidal field at plasma axis is approximately 5 T,
(2) dimension of coil bore is approximately 6 x 9 m,
(3) superconducting coil is cryogenically stabilized,
(4) unit reactor module includes two toroidal coils from the maintenance option,
(5) interval between two coils has the area enough for neutral beam injection,
(6) toroidal field ripple is less than $\pm$ 1.0 %.

It is desirable that the toroidal field magnet is as highly reliable as possible from the view point of plant availability. Every component should be designed on the basis of this consideration.

The twisted multifilamentary Nb_3S_n superconducting composite is used, and the stabilizer is copper. The toroidal field at the palsma axis is 5 T, providing 9.6 T of the maximum field at the coil. The coil bore is 6.0 x 9.0 m, and the coil shape is constant tension D-shape. The toroidal field magnet consists of 12 coils, considering the necessity for effective neutral beam injection and adequate shielding, 12 coils are arranged at an equal angular interval of 30°, and the maximum toroidal field ripple in the plasma region is ±0.75 %. The coil outer dimension is 8 m width X 11.1 m height. The cross section area of the coil is $\sim$ 1.2 m^2, resulting in an overall average current density of 8.8 ampere/mm^2.

Modified constant tension D-shape is chosen, to optimize a stress distribution and minimize a bending stress in coil structure. The length of the coil straight section is 5.6 m, and the inward centering force is ~ 32,000 ton/coil. The centering force is supported by wedged inner portion of the 12 coils. The hoop force is supported by stainless steel structure of the coil. The maximum stress in the structure is $\sim$ 35 kg/mm^2. The main design characteristics of the toroidal field magnet are shown in Table 4.1.1.

The current leads of each coil are connected as shown in previous works (1)(2). This power supply system is chosen from the view point

of coil protection. An energy dump resistor is connected in series with the windings. The induced voltage is lower than 5 kV by earthing the middle of windings.

The vacuum chamber of the toroidal field magnet is assembled in unity with all coils. A bird-cage flange is set beforehand at the centre of the machine, and each two-coil module is transported inward and pushed to the flange, as shown in Fig. 4.1.1. A metal gasket between the flange and the module keeps vacuum at the level of 10^{-4} Torr.

References

(1) Fusion Reactor System Laboratory: "Design study of superconducting toroidal field magnet for tokamak experimental fusion reactor" (in Japanese), JAERI-M 7298 (1977)

(2) Fusion Reactor System Laboratory: "Safety Analysis of Superconducting Toroidal Field Magnet for Tokamak Experimental Fusion Reactor", (in Japanese) JAERI-M 7963 (1979).

Table 4.1.1 Main Parameters of Toroidal Field Magnet

Number of coils	12
Major radius	5.0 m
Coil bore	6 x 9 m
Coil thickness	0.9 ~ 1.1 m
Coil width	1.08 m
Magnetic field at plasma center	5 T
Maximum field at coil	9.6 T
Maximum ripple in plasma region	0.75 %
Magnetomotive force	125 MAT
Superconductor	Nb_3S_n
Stabilizer	Cu
Superconducting composite	Fine-multi twisted

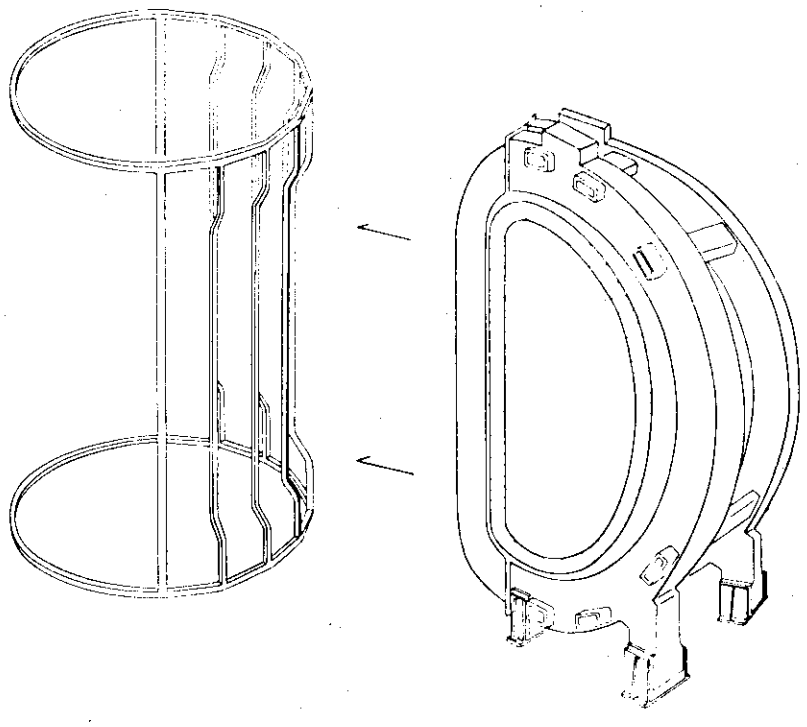

Fig. 4.1.1 Magnet Cryostat Assembling

4.2 Design of the Poloidal Field Coils

4.2.1 Design Principles

Poloidal field coil system is designed based on the following principles.

(1) Easy construction and repairing by remote handling.

(2) Reduction of electric power and energy required for the poloidal field coils.

(3) Reduction of heat dissipation due to magnetic field change in the superconducting toroidal field coils.

Naturally above principles can not be realized simultaneously, therefore some optimization should be carried out under the above conditions. The top priority exists on the principle (1), in the design of INTOR poloidal field coil system.

Besides the above principles, attention is paid to the followings.

(1) Overall current density of the poloidal field coils averaged over the cross section, which includes cooling and supporting structure, is set at 20 A/mm^2, which seems to be realized on the now existing superconducting technology.

(2) Shaping component of the magnetomotive force of each coil is decided in such a way that the cross section of any particular coil should not be excessively large. If not so, large electric power is required for that coil and the controllability of that coil will be deteriorated. Moreover evil influence is exercised upon the neighbouring part of the superconducting toroidal coils due to strong magnetic field and large magnetic field change of the coils concerned.

Assessment of the hybrid poloidal field coil system of INTOR is summarized in Table 4.2.1

4.2.2 Design Results

(1) Coil locations

Coil locations are shown in Figure 4.2.1. In this design hybrid poloidal field coil system is employed to reduce the number of coils. Moreover less electric power is required for the hybrid coil system.

(2) Shaping component of the magnetomotive forces

To attain D-shape plasma equilibrium with ellipticity, κ, of 1.5 and rectangularity, Δ, of about 0.4, shaping components of the magnetomotive forces of each coil are adjusted properly based on the principles described above.

The results are listed in Table 4.2.2. Shaping component supplies about 25 V-s magnetic flux. Magnetic field configuration and equi-B surfaces are shown in Figures 4.2.2 and 4.2.3 for both with and without divertor.

(3) Transformer component of the magnetomotive forces

Ohmic heating coils are so designed as to minimize the magnetic field leakage into the plasma region, and the same way is employed in the design of the hybrid poloidal field coils.

Designed values listed in the 6th column of Table 4.2.2 are decided to attain minimum field leakage.

Magnetic field configurations and equi-B surfaces are shown in Figures 4.2.4 and 4.2.5. The maximum field is about 5 T.

(4) Free boundary equilibrium calculation

Free boundary plasma equilibrium calculations were carried out and the results are shown in Figure 4.2.6 for both cases with and without divertor. The case with divertor requires more magnetomotive forces and electric power.

(5) Separatrix vibration for divertor heat load reduction[1)]

Conventional divertors receive large heat flux along scrape-off layer of main plasma which seems to be unable to be removed. To avoid this difficulty, separatrix should be swung back and force with some frequency which is acceptable in the view point of electric power required for swinging. Separatrix swinging is made by changing the current No.9 coil.

(6) Poloidal magnetic field and lateral force along the toroidal field coils

To reduce the heat dissipation in the superconducting toroidal field coils, it is advantageous that the poloidal magnetic field along the toroidal field coils is as small as possible.

Magnetic field distribution along both inner and outer perimeter of the toroidal field are shown in Figure 4.2.7. Lateral forces and moments acting on the toroidal field coils are shown in Figure 4.2.8.

Future Investigation

Some problems to be studied in the future investigation are described below.

(1) Method of plasma position and shape control during start-up.

(2) Evaluation of heat dissipation in the superconducting toroidal field coils, and the development of the method for effective heat removal. Detailed design which produces less heat should be carried out.

(3) Precise stress analysis should be made priori to the next step detail design.

Reference

1) Y. Shimomura, K. Sako, K. Shinya : "Some Considerations of Ash Enrichment and Ash Exhaust by a Simple Divertor", JAERI-M 8294 (1979)

Table 4.2.1 Assessment of the INTOR Poloidal Field coils

	Advantages	Disadvantages
Hybrid Coil	∘Reduction of electric power and energy ∘Simple structure	∘Necessity of sophisticated control method
Outside of TFC	∘Easy construction and repairing	∘Need more electric power ∘Bad controllability
Super-conducting	∘Reduction of electric power and energy	∘Complicated structure ∘Upper limit of B and $\dot{B}$

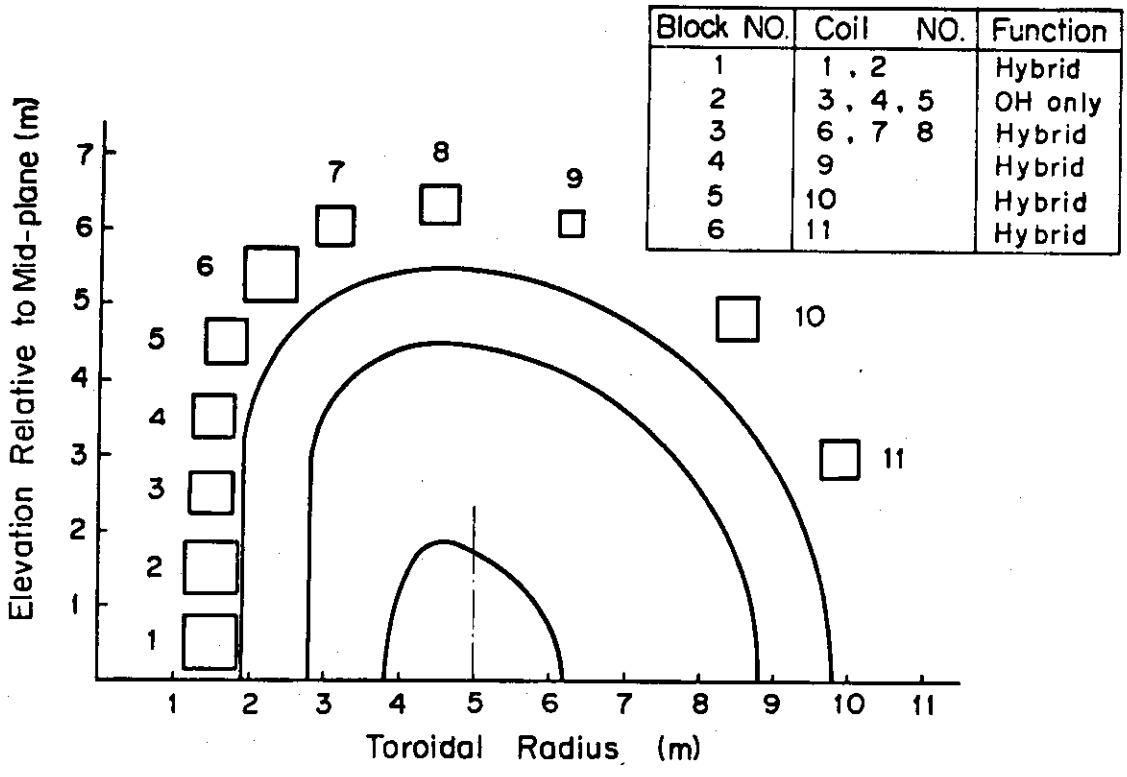

Fig. 4.2.1 INTOR Hybrid Poloidal Coil Locations

Table 4.2.2 INTOR Poloidal Field Coil Locations and Maximum Ratings

Coil No.	Block No.	R (M)	Z (M)	N #	Transformer Component (MAT)	Shaping Component (MAT)	Total (MAT)	Shaping Component (MAT)	Total (MAT)
						with divertor		without divertor	
1	1	1.5	0.5	1	-3.68	-2.34	-6.02	-1.95	-5.63
2	1	1.5	1.5	1	-3.68	-2.34	-6.02	-1.95	-5.63
3	2	1.5	2.5	1	-3.60	*****	-3.60	*****	-3.60
4	2	1.525	3.5	1	-3.60	*****	-3.60	*****	-3.60
5	2	1.675	4.5	1	-3.60	*****	-3.60	*****	-3.60
6	3	2.25	5.4	2	-1.72	10.0	8.28	8.0	6.28
7	3	3.1	6.05	1	-0.86	5.0	4.14	4.0	3.14
8	3	4.5	6.35	1	-0.86	5.0	4.14	4.0	3.14
9	4	6.25	6.1	1	-0.15	+0.0 -1.0	-0.15 -1.15	*****	0.15
10	5	8.5	4.85	1	-0.10	-5.17	-5.27	-3.29	-3.39
11	6	9.9	3.0	1	-0.15	-1.98	-2.13	-2.87	-3.02

Plasma current I_p at the flat-top is 4.7 MA.

#.. N is a ratio of the coil turns in the same block.

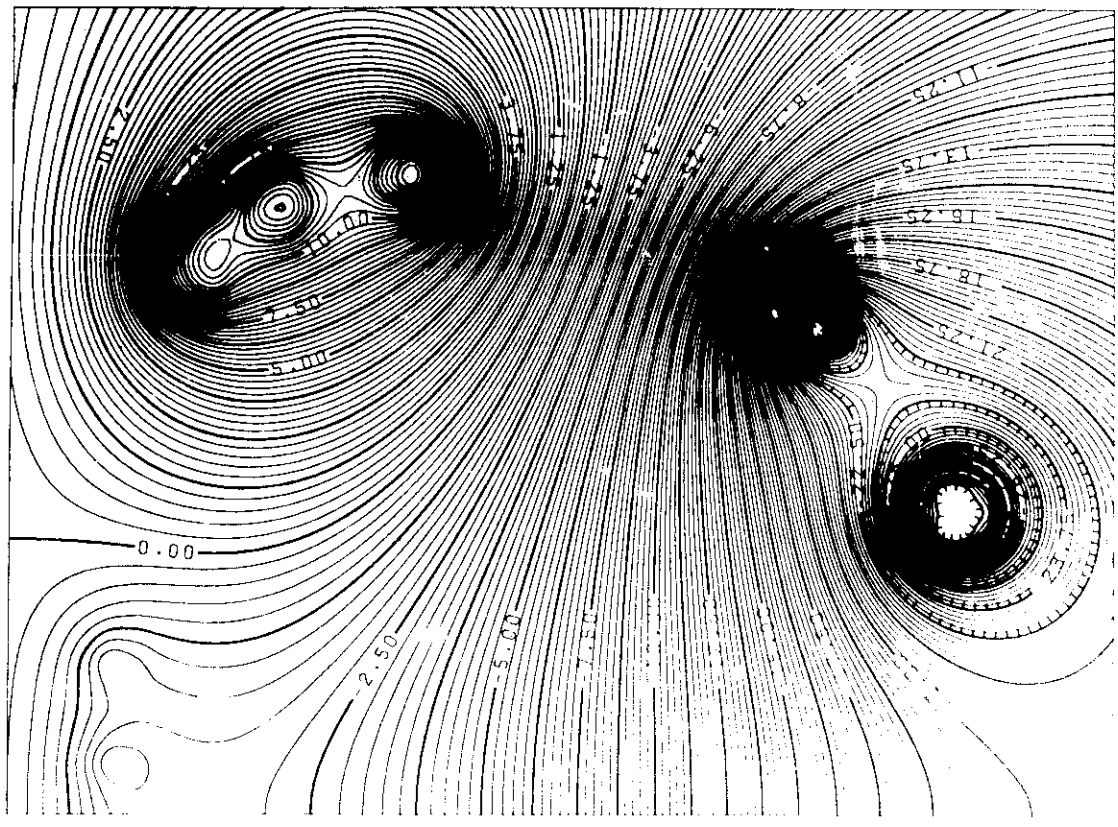

Fig. 4.2.2 (a) Magnetic field configuration produced by shaping component of the hybrid poloidal field coils; non-divertor case.

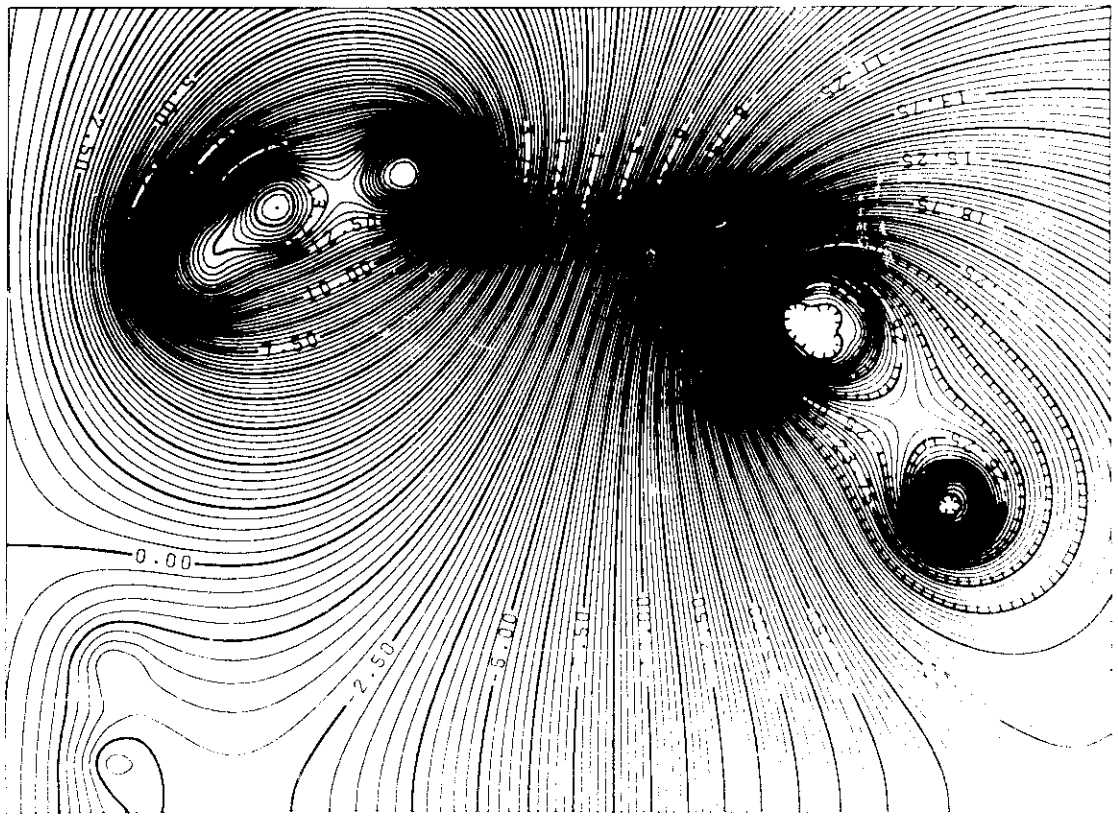

Fig. 4.2.2 (b) Magnetic field configuration produced by shaping component of the hybrid poloidal field coils; divertor case.

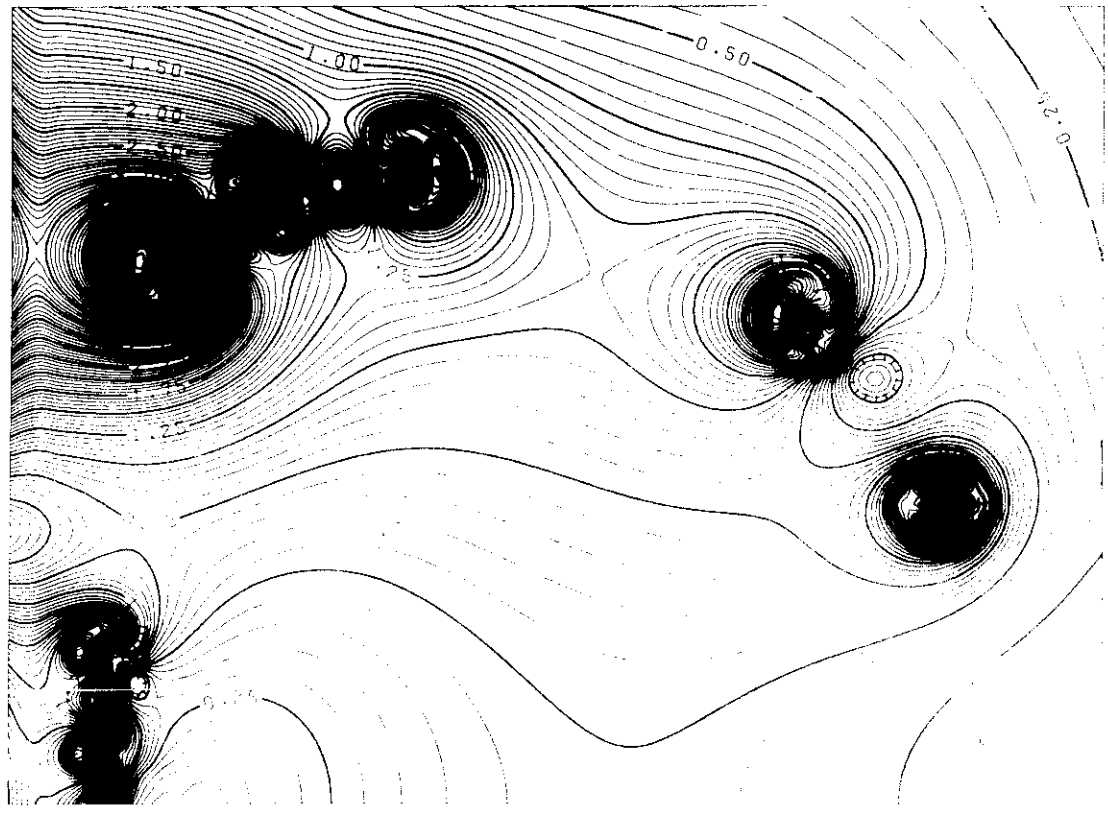

Fig. 4.2.3 (a) Equi-B surface of the equilibrium field without divertor.

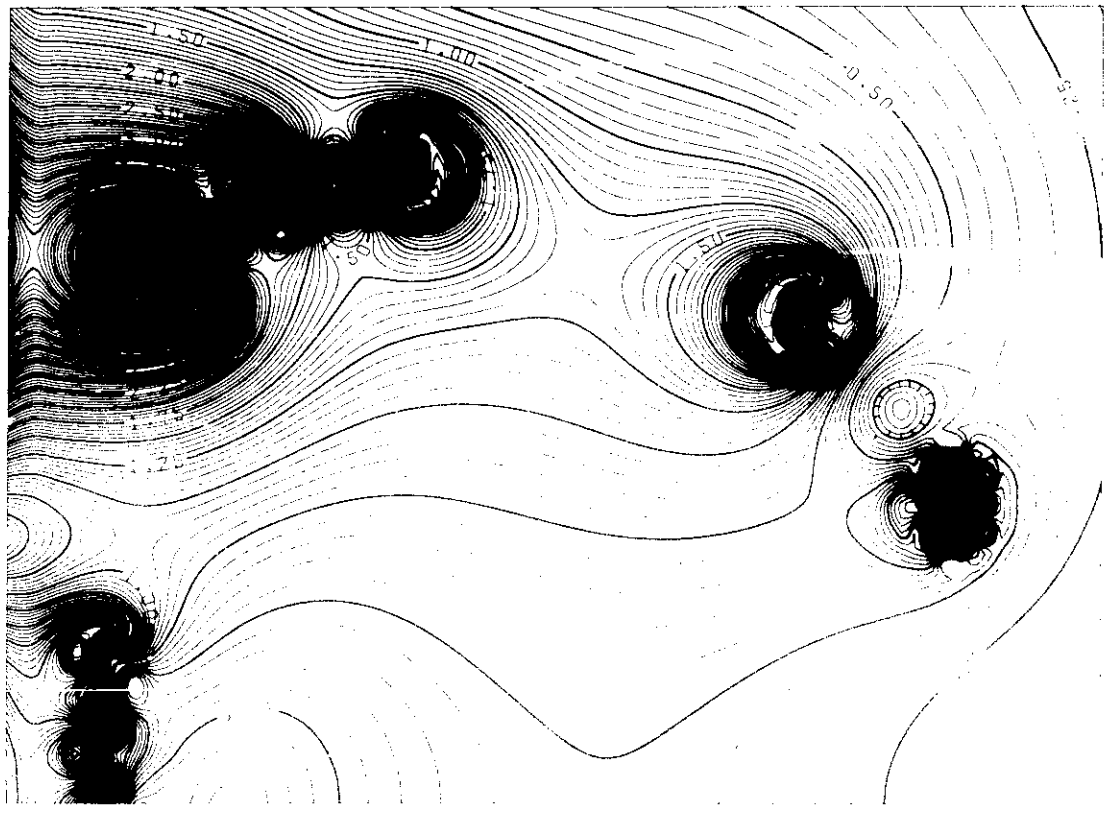

Fig. 4.2.3 (b) Equi-B surface of the equilibrium field with divertor.

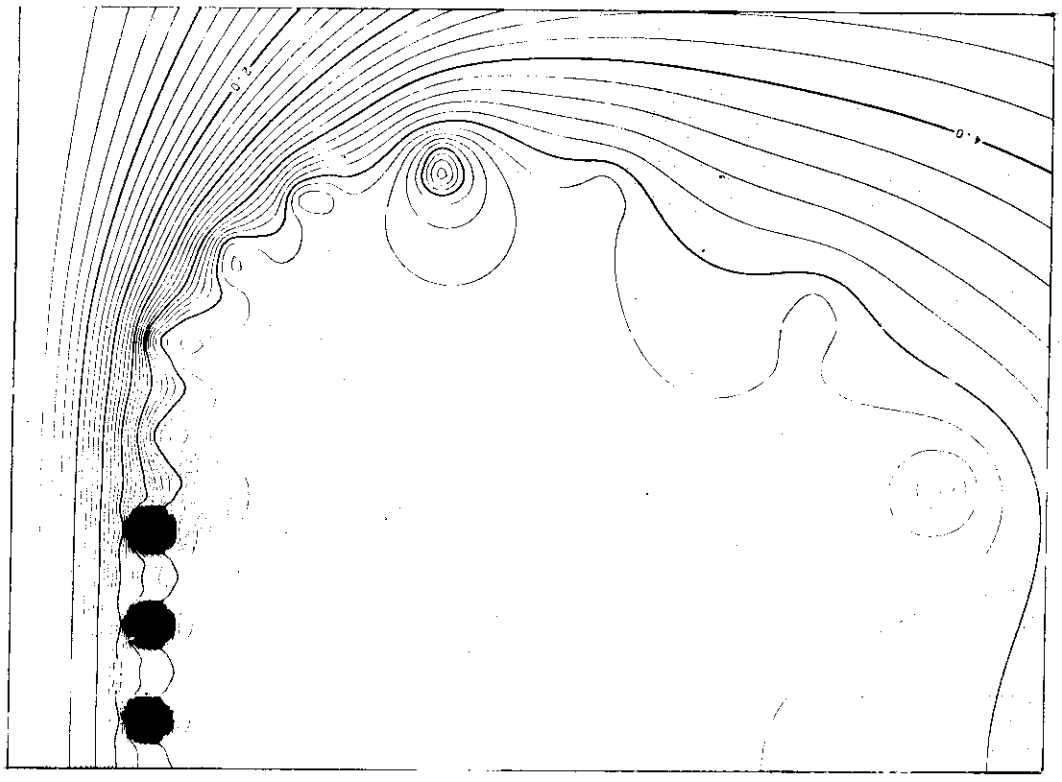

Fig. 4.2.4 Magnetic field configuration produced by transformer component of the hybrid poloidal field coils.

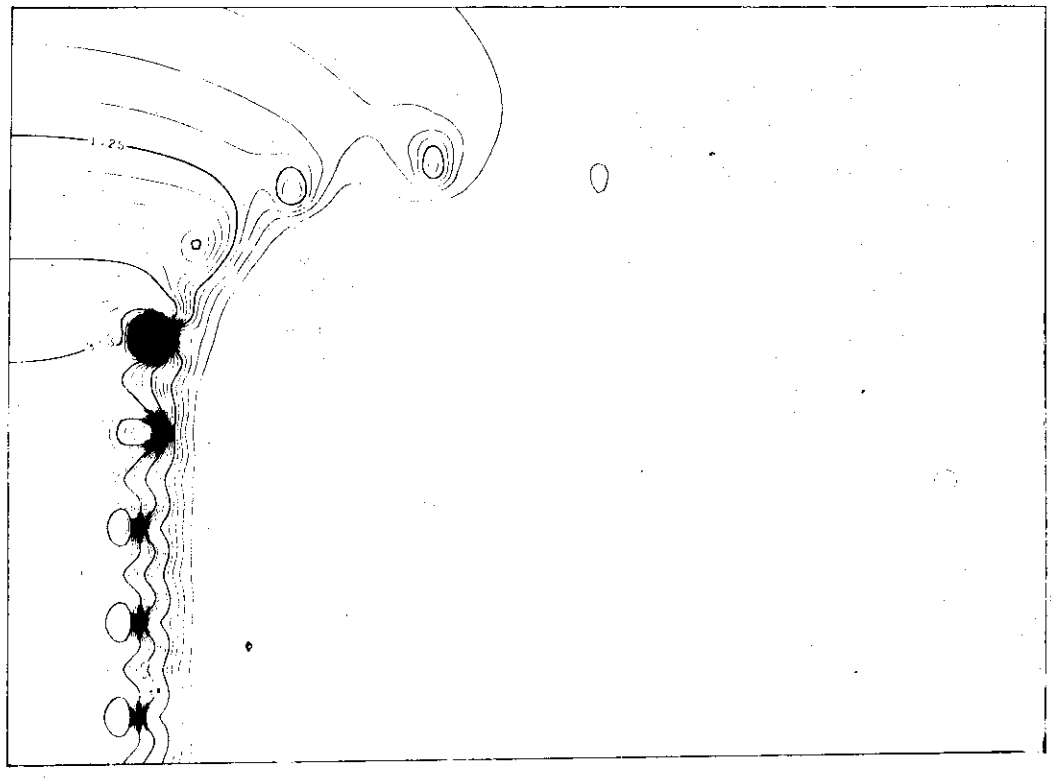

Fig. 4.2.5 Equi-B surface of the magnetic field configuration produced by transformer component.

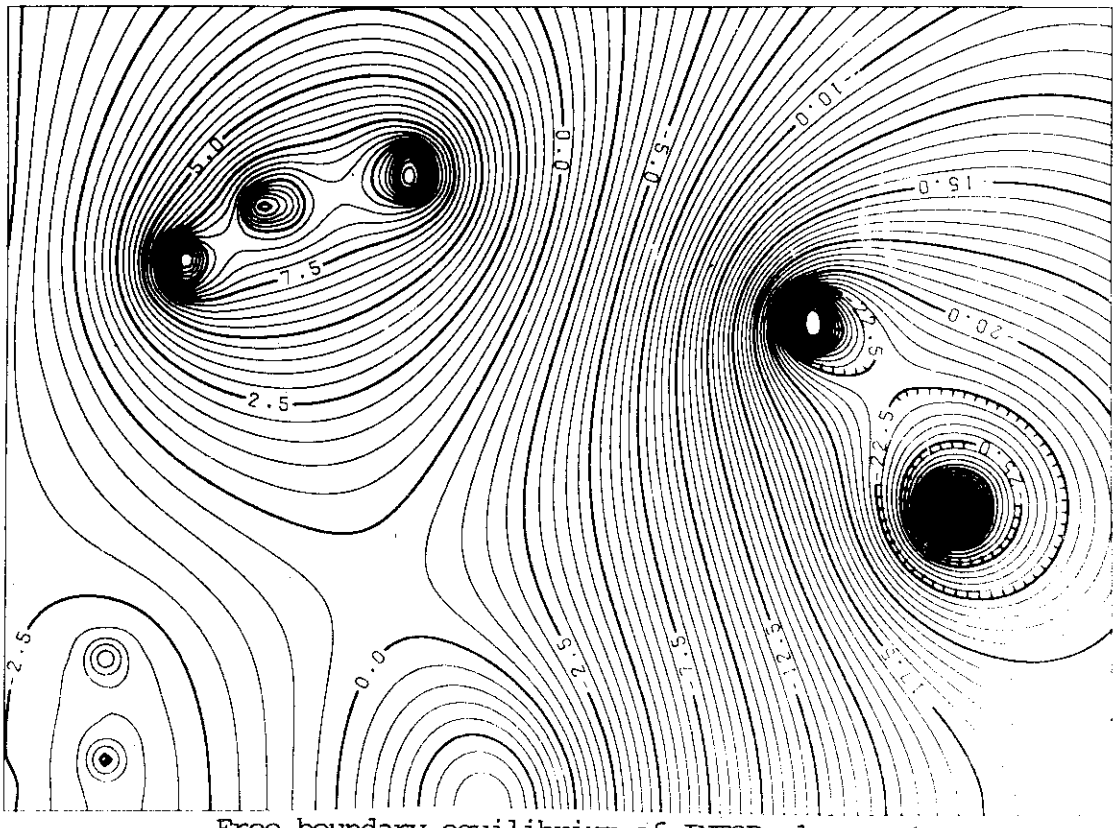

Fig. 4.2.6 (a) Free boundary equilibrium of INTOR plasma without divertor configuration.

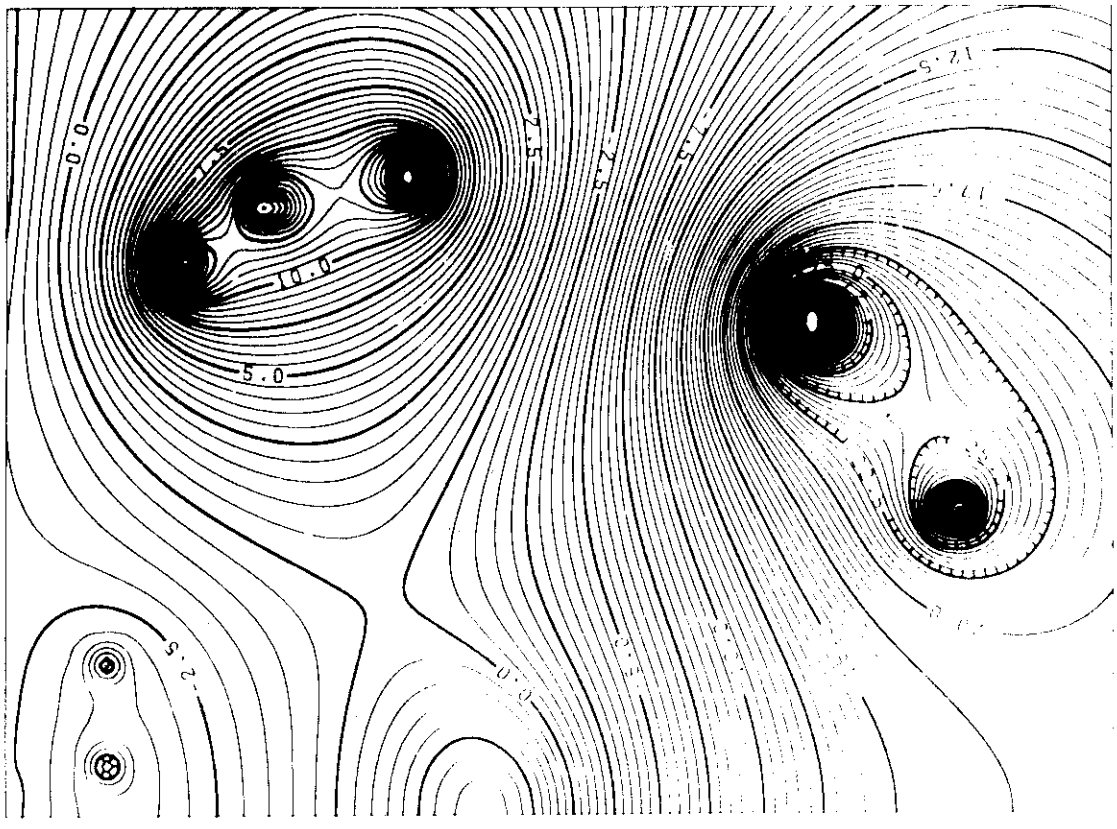

Fig. 4.2.6 (b) Free boundary equilibrium of INTOR plasma with divertor configuration.

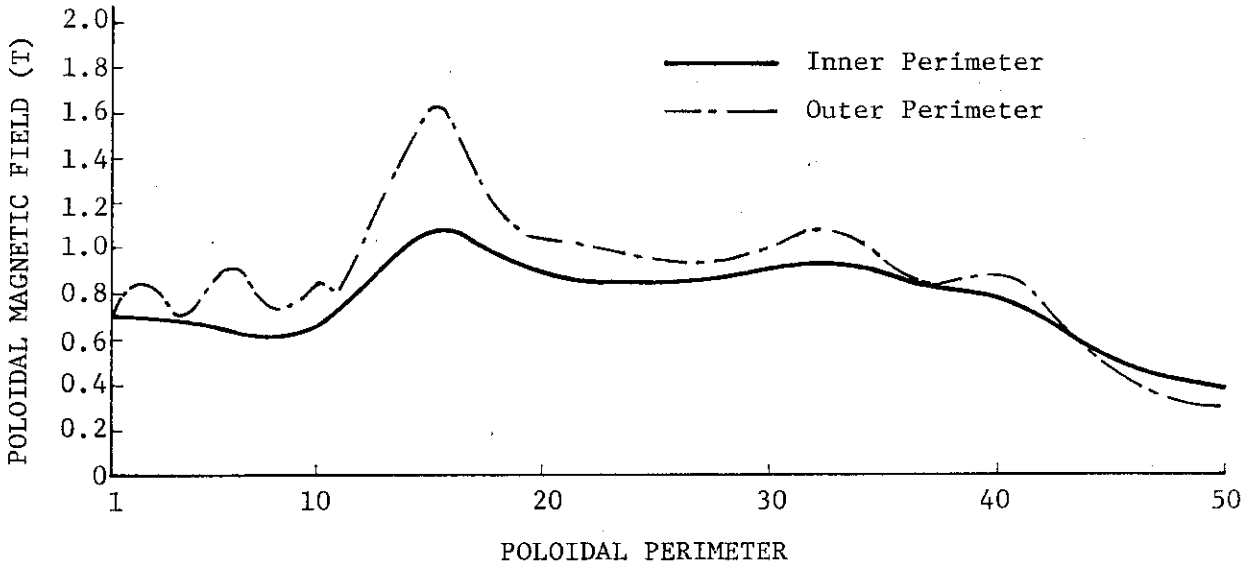

Fig. 4.2.7 Poloidal magnetic field distribution along poloidal perimeter of the toroidal field coil

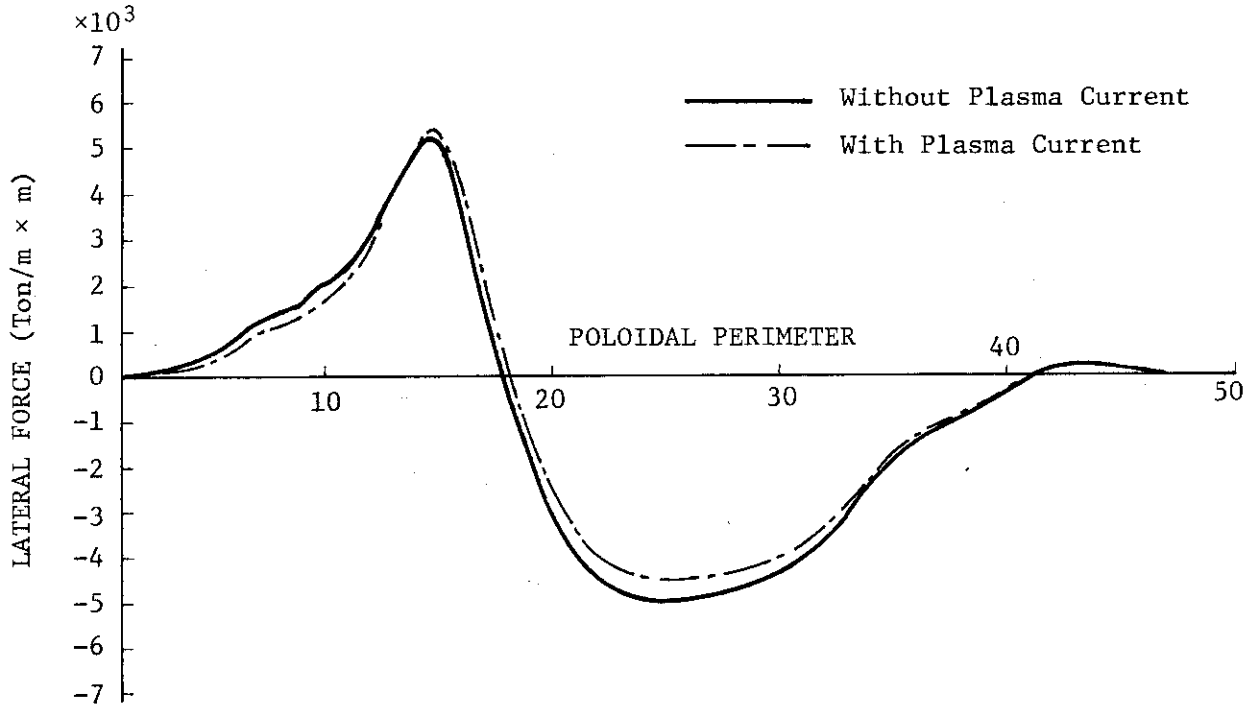

Fig. 4.2.8 Lateral force distribution along poloidal perimeter of the toroidal field coil

5. Neutral Beam Injector

The concept of NBI shown in Figures 1.2 and 1.3 was developed from the NBI design for JXFR. The injectors are to be installed on the ports in the 4 modules out of the 6. There are 6 beams per port giving the total of 24 beams to supply 50 MW. The required injection power per port becomes 3 MW by leaving a margin against the failure. The angle of injetion is $\pm$ 15° in the horizontal direction and deviation in the vertical direction is 0° and $\pm$ 7°. The necessity of the energy convertor shown in the figures needs further examination in view of the capacity of the power supply and the complexity of the whole injector system. Following items must be pursued concerning the NBI :

(1) To make them more compact and high powered.

(2) The design must be refined taking into account the repair and maintenability.

6. Reactor Cooling System

A reactor cooling system is formed with three systems which cool outer blanket (tritium breeding), inner blanket (non-breeding) and cooling panel. The outer blanket cooling system has 2 lines, the inner blanket cooling system has 1 line and the cooling panel has 2 lines.

An electric power will be produced in the outer blanket cooling system and cooling panel, but not in the inner blanket cooling system. Intermediate loops to protect a tritium release are provided in each system.

A helium gas is used for the cooling system of the outer blanket (primary and secondary loops) and the cooling panel (primary and secondary loops). A pressurized water is used for the cooling system of the inner blanket.

Design parameters of the reactor cooling system and heat load of each system are shown in Tables 6.1 and 6.2, respectively. The flow sheet of the reactor cooling system is shown in Fig. 1.4.

5. Neutral Beam Injector

The concept of NBI shown in Figures 1.2 and 1.3 was developed from the NBI design for JXFR. The injectors are to be installed on the ports in the 4 modules out of the 6. There are 6 beams per port giving the total of 24 beams to supply 50 MW. The required injection power per port becomes 3 MW by leaving a margin against the failure. The angle of injetion is $\pm$ 15° in the horizontal direction and deviation in the vertical direction is 0° and $\pm$ 7°. The necessity of the energy convertor shown in the figures needs further examination in view of the capacity of the power supply and the complexity of the whole injector system. Following items must be pursued concerning the NBI :

(1) To make them more compact and high powered.

(2) The design must be refined taking into account the repair and maintenability.

6. Reactor Cooling System

A reactor cooling system is formed with three systems which cool outer blanket (tritium breeding), inner blanket (non-breeding) and cooling panel. The outer blanket cooling system has 2 lines, the inner blanket cooling system has 1 line and the cooling panel has 2 lines.

An electric power will be produced in the outer blanket cooling system and cooling panel, but not in the inner blanket cooling system. Intermediate loops to protect a tritium release are provided in each system.

A helium gas is used for the cooling system of the outer blanket (primary and secondary loops) and the cooling panel (primary and secondary loops). A pressurized water is used for the cooling system of the inner blanket.

Design parameters of the reactor cooling system and heat load of each system are shown in Tables 6.1 and 6.2, respectively. The flow sheet of the reactor cooling system is shown in Fig. 1.4.

Table 6.1 Design Parameters of the Reactor Cooling System

Inlet and outlet helium temperature of outer blanket cell	:	250/550°C
Inlet and outlet helium temperature of cooling panel	:	200/300°C
Inlet and outlet water temperature of inner blanket	:	60/100°C
Helium pressure of outer blanket (primary/secondary; 40φ pipe (outlet))	:	30/50 ata
Helium pressure of cooling panel (primary/secondary; 14φ tube))	:	70/75 ata
Water pressure of inner blanket (primary/secondary; 10φ tube)	:	5/7 ata
Condensing temperature and pressure*	:	50°C,0.126 ata
Turbine efficiency	:	80 %
Power transfering efficiency x generator efficiency	:	95 %
Electric power (gross)	:	53.8 MW
Circulator power	:	11.4 MW

* Using a dry-type condensor

Table 6.2 Heat loads of cooling systems

Cooling system	Heat load (MW)
Cooling panel	130
Inner blanket	95
Outer blanket	190
Inner shield	6
Outer shield	5

7. Repair and Maintenance

From the experience of the JXFR design, if the reactor itself can be disassembled, the extraction and replacement of the reactor module seems to be feasible from engineering point of view. One of the critical problems in the disassembly of the reactor is cutting and reconstructing of the vacuum vessel (See Section 4.1).

The module extraction scheme requires the large task of disassembling the reactor even for a partial repair. However, the merits of this scheme are that every components may be repaired or replaced, and that the inspection of the reassembled state is simplified due to modularization.

The choice of repair and maintenance scheme greatly influences the overall reactor design. It is difficult to select which scheme to adopt at this early stage of the design. Whichever scheme it may be, it is important to establish a workable one. In the case of a design which satisfies the INTOR guiding parameters and breeds tritium at a same time, it is difficult to take the blanket out for repair without removing shield and toroidal field coils. In such a case, the modular concept employed in the design of JXFR seems to be the only solution. Therefore, this scheme was also adopted for the INTOR-J design and hence the maintenance procedure will be similar to that of the JXFR. It seems reasonable for the INTOR to be built in near future to have every components repairable.

As for the parts with high failure probability such as the neutralizer plate for divertor, it is desirable to be able to repair them without the disassembly of the reactor.

ACKNOWLEDGMENT

The authors are greatly indebted to Drs. S. Mori and Y. Obata for their encouragement. They also thank deeply to the people in JAERI who participated in the INTOR-J program.

They would like to acknowledge deeply the people from the industries who participated in the design study; Special thanks are extended to the people in Kawasaki Heavy Industries, Ltd. for their enthusiastic contributions on the design of blanket structure and its cooling system.